GRAVITY AND MAGNETIC STUDY OF NORMALLY AND REVERSELY POLARIZED INTRUSIONS, MENOMINEE COUNTY, MICHIGAN

Thesis for the Degree of M. S.

MICHIGAN STATE UNIVERSITY

PEDRO LEON TORRES

1976

ABSTRACT

GRAVITY AND MAGNETIC STUDY OF NORMALLY AND REVERSELY POLARIZED INTRUSIONS, MENOMINEE COUNTY, MICHIGAN

By

Pedro Leon Torres

Aeromagnetic anomalies of positive and negative magnetic amplitude were investigated by surface gravity and magnetic methods. This leads to an interpretation of such parameters as total mass of the anomalous bodies, density contrast, volume, depth, magnetic susceptibility, remanent and induced magnetization components, Koenigsberger ratio, and possible magnetite content. The main purpose was to investigate the remanent magnetization and its polarity by indirect means, using gravity to define the size and depth of the two anomalous bodies, and magnetics to interpret polarity and magnitude of remanence of the two intrusions. The anomalies are adjacent, have roughly concentric patterns, and have high and low magnetic intensities. They are suggestive of stock-like intrusive bodies in the basement rock. Such a study of localized intrusions usefully complements other work that has been done on interpretation of dike-like, or other "two-dimensional" features.

Ground gravity and magnetic surveys of the area in the southern Upper Peninsula of Michigan (Menominee County) were carried out from November, 1975 to January 1976. One hundred and fifty-two gravity stations were occupied with a station spacing from a half mile in swamp areas to a quarter mile on the central and western portion of a 16 square mile grid pattern. One hundred and thirty seven magnetic stations were occupied with a station spacing similar to the gravity survey. Vertical ground magnetic and Bouguer gravity maps of the area surveyed were prepared after applying the normal corrections. The vertical-intensity ground magnetic map indicated the presence of a magnetic high and a magnetic low which coincided with two well marked gravity highs. Only fragmentary direct geologic information was available on the basement complex in this part of northern Michigan, because of overburden of glacial drift, Paleozoic sedimentary rock, and poorly distributed basement drill holes. However, depth to the basement surface was estimated using the geophysical methods. The few well logs from drilling confirmed that the basement surface under the area surveyed was not deeper than 200 feet for both anomalies. The bottom of the possible causative bodies can be modelled as being on the order of 10,000 feet.

These anomalies were believed to be originating from mafic intrusives possibly coming from PreKeweenawan

or Keweenawan igneous activity. The interpretation of the anomalies was begun by curve fitting various size vertical cylinders with an assumed minimum density contrast of 0.3 gm/cm^3 and a maximum of 0.45 gm/cm^3. This resulted in a fit of the sizes for the southern anomalous body (3.57 milligals) of 17.7 cubic kilofeet, and for the north-central anomalous body (4.47 milligals) of 25.2 cubic kilofeet. The mass excess was 2.15×10^{14} gm for the first one, and 3.06×10^{14} gm for the second one.

On the basis of well logs from drilling, a "Fence Diagram" was constructed and a maximum depth to the basement structure was calculated to be 200 feet. Induced and remanent magnetization were calculated by the formula $J = Ji \pm Jr$, where Ji is the intensity of magnetization due to induction by the earth's present magnetic field, and Jr is the natural remanent magnetization. The calculated Jr was stronger than Ji in both cases. The susceptibility contrast assumed for both bodies was 1.9×10^{-3} e.m.u/cm^3. The induced magnetization so calculated for both bodies gave a value of 1.05×10^{-3} e.m.u/cm^3. The remanent magnetization for the positive anomalous body gave a value of 2.58×10^{-3} e.m.u/cm^3, and a value of -4.24×10^{-3} e.m.u/cm^3 for the negative one.

The Koenigsberger ratio, for the positive magnetic anomaly, was 2.46 and for the negative one, it was 4.04.

For this value the volume percent of magnetite was estimated as 2.9% and 3.5% for each respectively.

GRAVITY AND MAGNETIC STUDY OF NORMALLY AND REVERSELY POLARIZED INTRUSIONS, MENOMINEE COUNTY, MICHIGAN

By

Pedro Leon Torres

A THESIS

Submitted to
Michigan State University
in partial fulfillment of the requirements
for the degree of

MASTER OF SCIENCE

Department of Geology

1976

ACKNOWLEDGMENTS

It is with sincere appreciation that thanks are extended to Dr. Robert S. Carmichael, my thesis Chairman, for his stimulation, enthusiasm, assistance, and criticism during the course of this study.

Thanks are also extended to Drs. F. W. Cambray and J. W. Trow for helpful suggestions and critical review of the manuscript.

The author wishes to express his sincere gratitude to Dr. R. Reed, who suggested this work, provided aeromagnetic maps of the area surveyed, and gave freely of his time for consultation.

I would also like to thank Dr. C. E. Prouty who provided literature and gave advice.

Special thanks are due to the invaluable assistance of Mr. N. E. Thurber, Mr. C. G. Ryan, and Mr. W. M. Phillips, Michigan State University students, for help with the measurement and some calculation of results of field work.

Special thanks are also due to the Venezuelan government (Ministerio de Obras Publicas), for scholarship support and financial assistance for this work.

Finally, I would like to extend my most sincere and deep appreciation to my wife, Migdalia.

TABLE OF CONTENTS

LIST OF FIGURES

Figure		Page

CHAPTER I

INTRODUCTION

The objective of this work is to study the nature of vertical-component positive and negative magnetic anomalies, in particular their remanent magnetizations, which are caused possibly by magnetiferrous or ferromagnesian intrusions in Menominee County of the Upper Peninsula of Michigan. The main reason to do this work was to investigate specifically the negative character (low magnetic anomaly) shown by the aeromagnetic map provided by Michigan Geological Survey (Department of the Interior, USGS, 1970). The total and vertical components of the field will give anomalies in opposition to those to be expected from the present field. Another subject of the present work will be to find the possible extent of magnetic rock deposits by making depth determinations to the top and bottom of theoretical cylindrical gravity models.

A sixteen-square-mile area of Menominee State Forest of the southern Upper Peninsula of Michigan was surveyed gravimetrically and magnetically (Figure 1) by

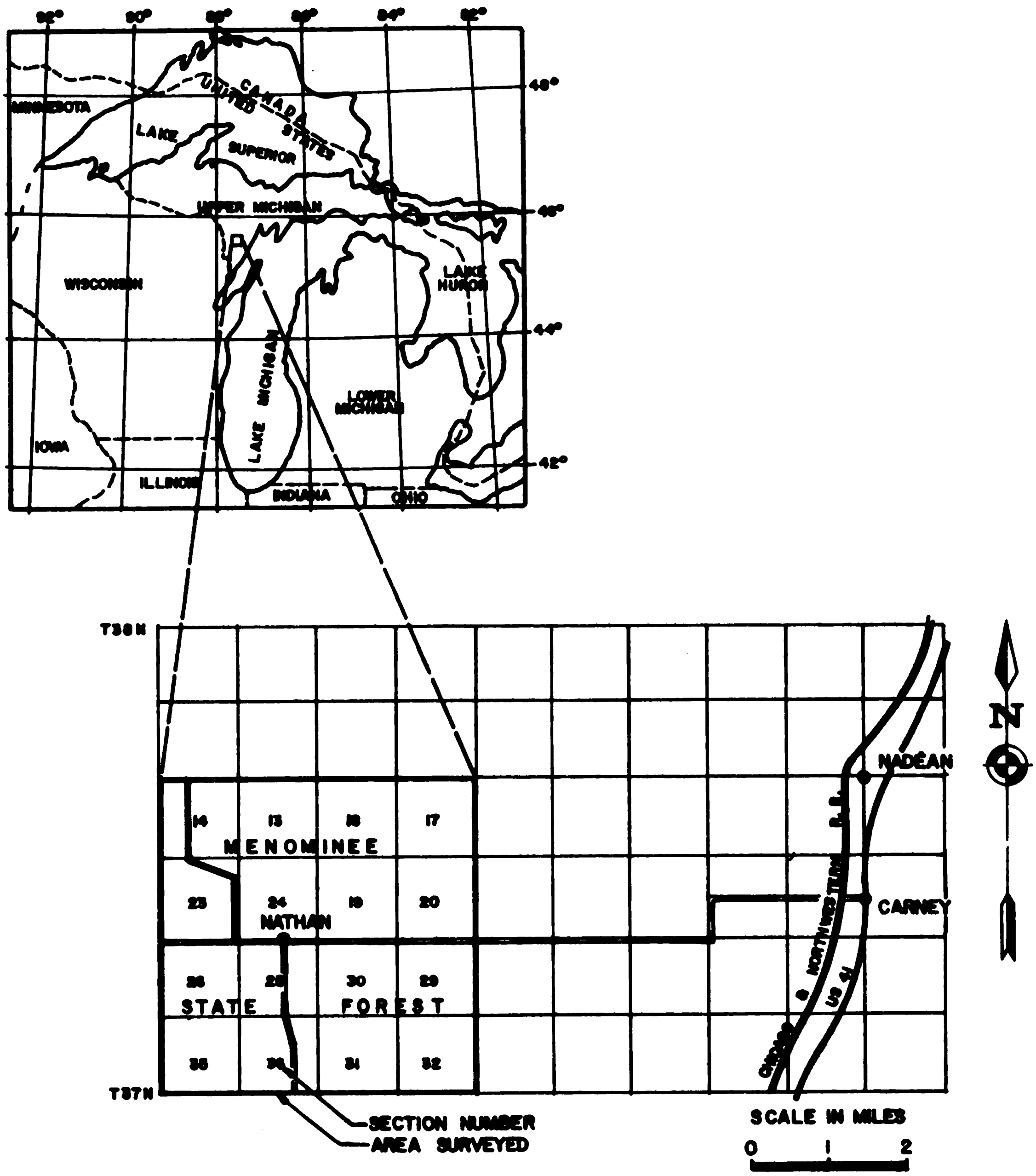

FIGURE. I INDEX MAPS

the writer in cooperation with Michigan State University students, in a project of geophysical interpretation.

The gravity and magnetic measurements were done concurrently. The gravity anomalies exhibited large positive values with respect to the regional trends drawn. These positive anomalies could be interpreted as intrusive masses of higher density than the surrounding basement rocks.

The position of the magnetic anomalies with respect to the position of gravity anomalies was observed to be very close to each other. However differences in size, center of maximum and minimum, and elongation were observed to be different, surely indicating the presence of a component of magnetization other than that induced by the earth's field. As the appreciable susceptibility and density contrast give rise to quite high anomalies, the gravity and magnetic method were adopted for the present work using a LaCoste Romberg gravimeter and a Fluxgate magnetometer. This proposed research will involve the application of gravity and magnetic geophysical exploration methods which will require assumptions about density and susceptibility contrast of rock material, and the relation of induced magnetization to the remanent magnetization with regard to polarity and intensity.

CHAPTER II

ACCESSIBILITY AND EXTENT OF THE AREA SURVEYED

That portion of the Menominee County covered by the accompanying index map (Figure 1) is located approximately between longitude 87° 39' W and 87° 44' W and latitude 45° 33' N and 45° 36' 30" N in the southern part of Menominee County of the Upper Peninsula of Michigan. The south part of the area is well delineated by the south line of T37N; Michigan. On the east side of the area, on section 29, is the "Wire Grass Lake" which is connected to the "Shakey River" to the south. At the north-northwest corner, there is another small river which together with the Shakey poorly drains the area (Figure 1-1, topographic map). The area surveyed from its starting point (base station N°1) is spatially located approximately five miles east from Carney, Michigan. It is, geomorphologically speaking, located in an area of sandy till moraines to the west and till sheets and till plains to the east, surrounded in its majority by lowland swamps. Close to Carney, Michigan (outside of the surveyed area) small drumlins were observed covering till sheets and till plains. Most of the area surveyed

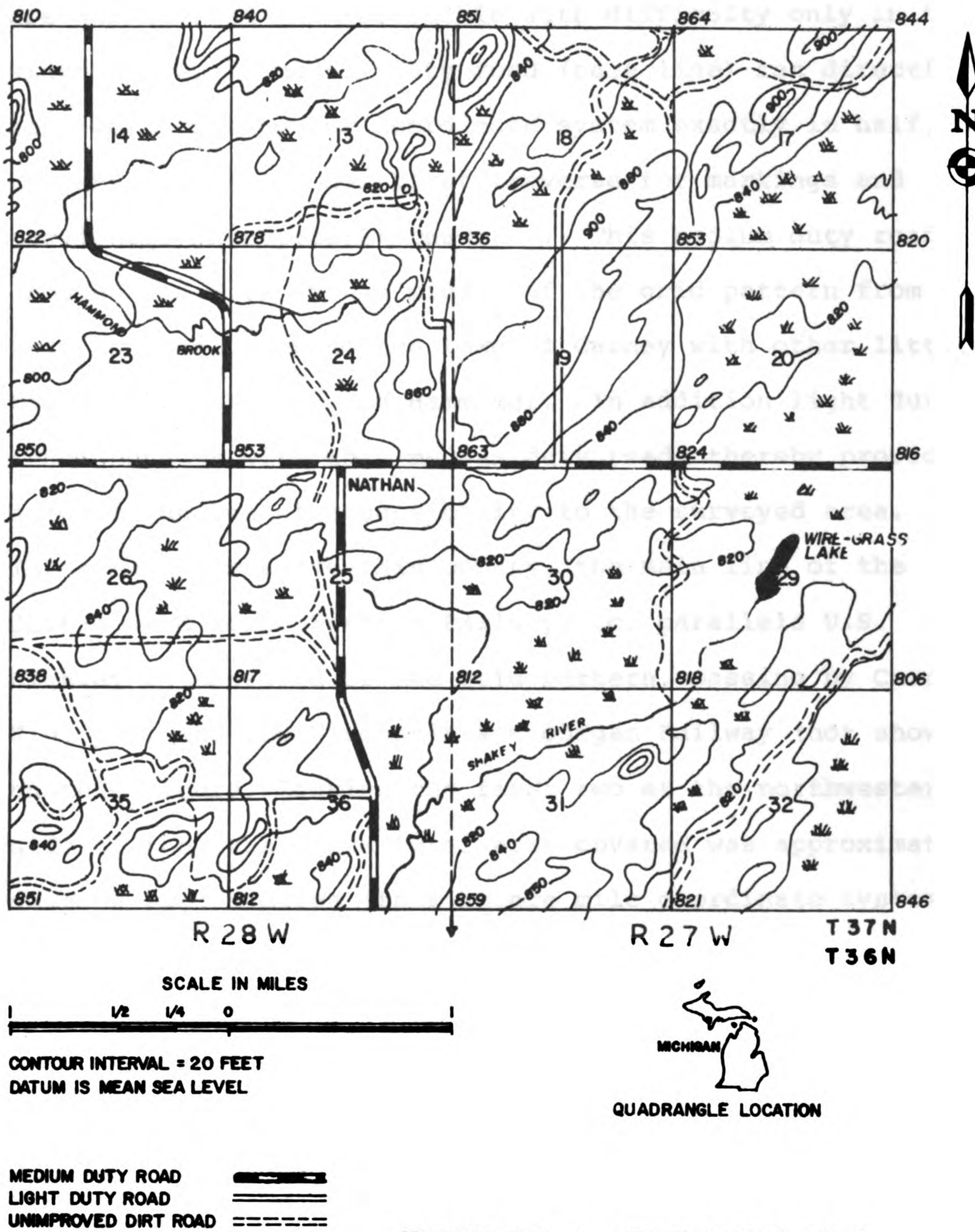

FIGURE I-1 TOPOGRAPHIC MAP

is accessible with the exception of low swamp areas that are uninhabited and accessible with difficulty only in the winter time. A medium duty road (base line) ran directly east-west cutting our coordinate system exactly in half, thereby serving as our first traverse for markings and gravimeter-magnetometer readings. This medium duty road crossed the area at the middle of the grid pattern from east to west, linking the town of Carney with other little towns (i.e., Nathan and Hammond). In addition light duty roads connect with this medium duty road, thereby providing a larger degree of accessibility to the surveyed area. Three railways serve this county, the main line of the Chicago and North-Western Railways Co. parallels U.S. Highway 2 (eastward of the grid pattern, passing by Carney, Fig. 1-1) and the Wisconsin & Michigan Railway (not shown on this figure) linking the first two at the northwestern side of the area. The total area covered was approximately sixteen square miles (four square mile coordinate system). The series of points, at which the geophysical measurements were taken, were marked off at regular intervals of 1/4 mile. However some points (therefore measurements) were inaccessible due to extremely dense wooded areas and swamps. Therefore, these areas necessitated the usage of 1/8 or 1/2 mile intervals from which to obtain data (Figures 2 and 3).

After doing all corrections, a Bouguer gravity and vertical magnetic maps (Figures 2-1 and 3-1) were drawn in order to make the interpretation and comparison with the total aeromagnetic map provided by the U.S. Geological Survey, which was flown at 500' above the earth's surface (Figure 4).

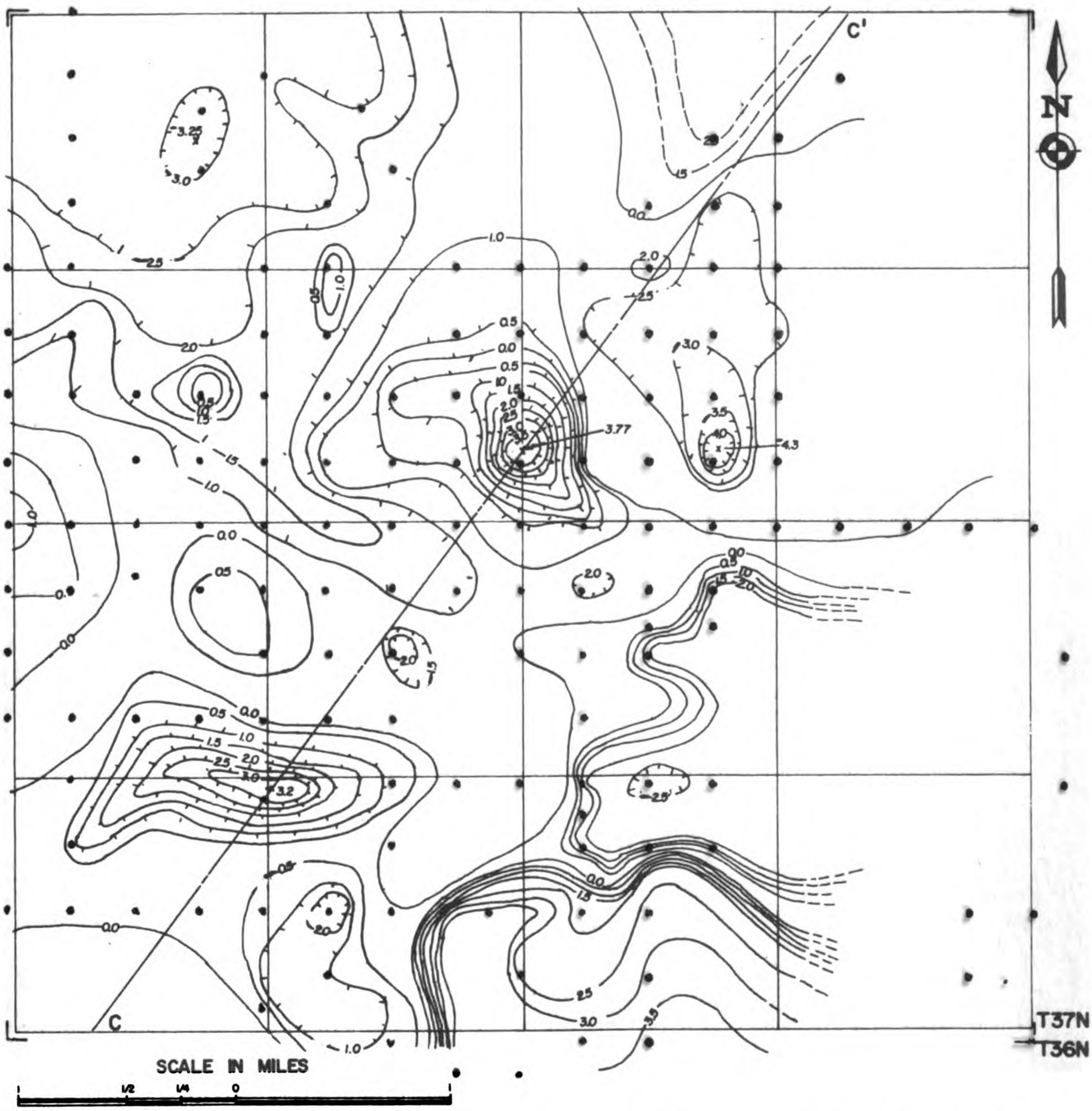

CONTOUR INTERVAL = 0.5mg.

CONTROL SHOWN BY EVERY 1/4 MILE WHICH REPRESENTS A GRAVITY STATION LOCATION SEE GRAVITY STATIONS – FIGURE 2

LEGEND

- 0.1 CONTOUR INTERVALS – MILLIGALS
- x 3.77 MEASURED MAXIMUM OR MINIMUM GRAVITY INTENSITY WITHIN CLOSED HIGH OR CLOSED LOW
- ---- INDICATES INCOMPLETE DATA
- INDICATES CLOSED LOW GRAVITY INTENSITY
- INDICATES CLOSED HIGH GRAVITY INTENSITY

BOUGUER GRAVITY MAP

• GRAVITY STATION

MENOMINEE COUNTY — NATHAN ANOMALIES

FIGURE 2-1

FIGURE 2. GRAVITY STATIONS

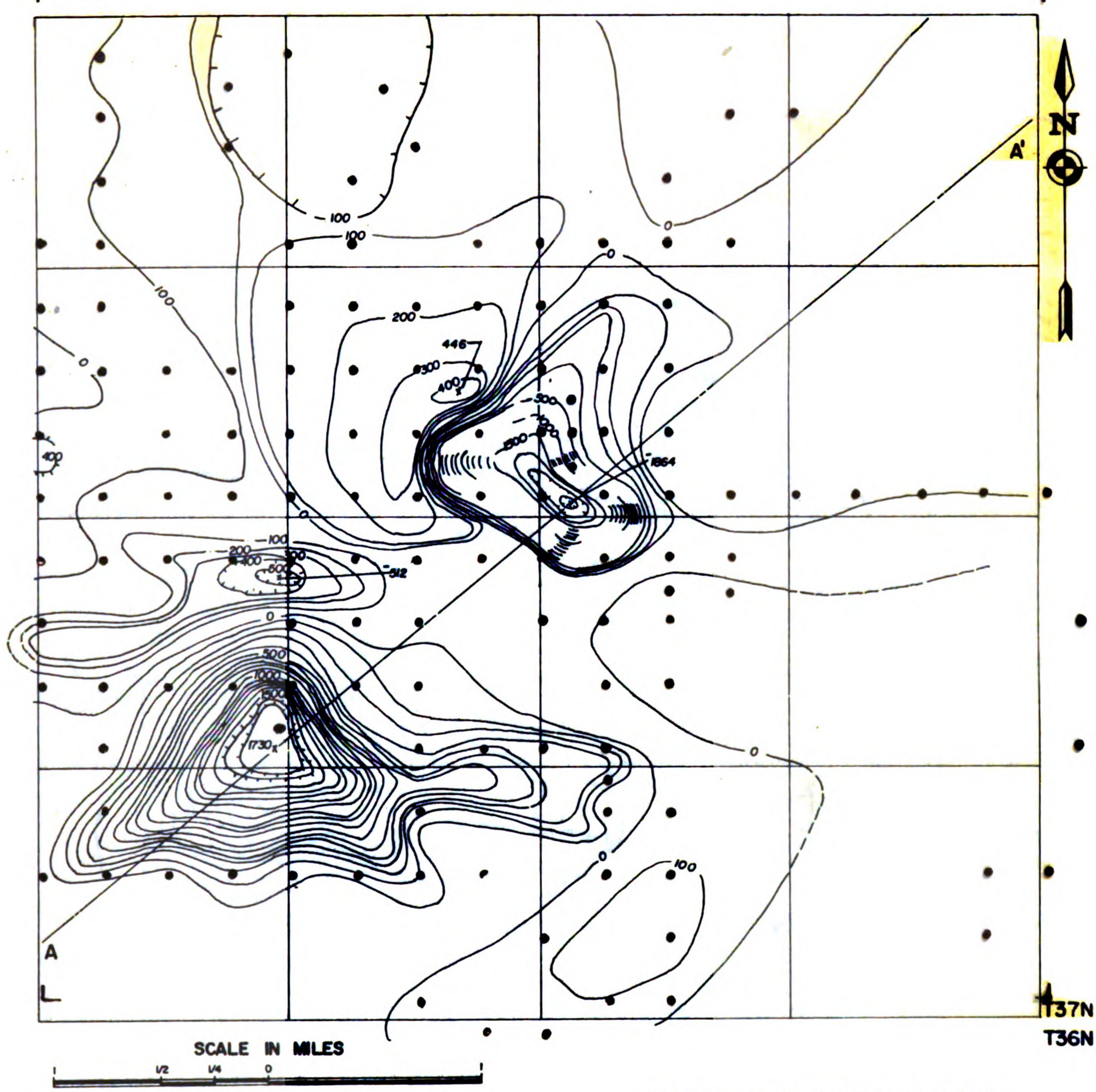

CONTOUR INTERVAL = 100 γ

CONTROL SHOWN BY EVERY 1/4 & 1/2 MILE WHICH REPRESENTS A MAGNETIC STATION LOCATION. SEE MAGNETIC STATIONS-FIG. 3

LEGEND

100 CONTOUR INTERVALS

MEASURED MAXIMUM OR MINIMUM MAGNETIC INTENSITY WITHIN CLOSED HIGH OR CLOSED LOW

INDICATES INCOMPLETE DATA

INDICATES CLOSED LOW MAGNETIC INTENSITY

INDICATES CLOSED HIGH MAGNETIC INTENSITY

MAGNETIC STATION

VERTICAL INTENSITY GROUND MAGNETIC MAP
MENOMINEE COUNTY — NATHAN ANOMALIES

FIGURE 3-1

FIGURE 3. MAGNETIC STATIONS

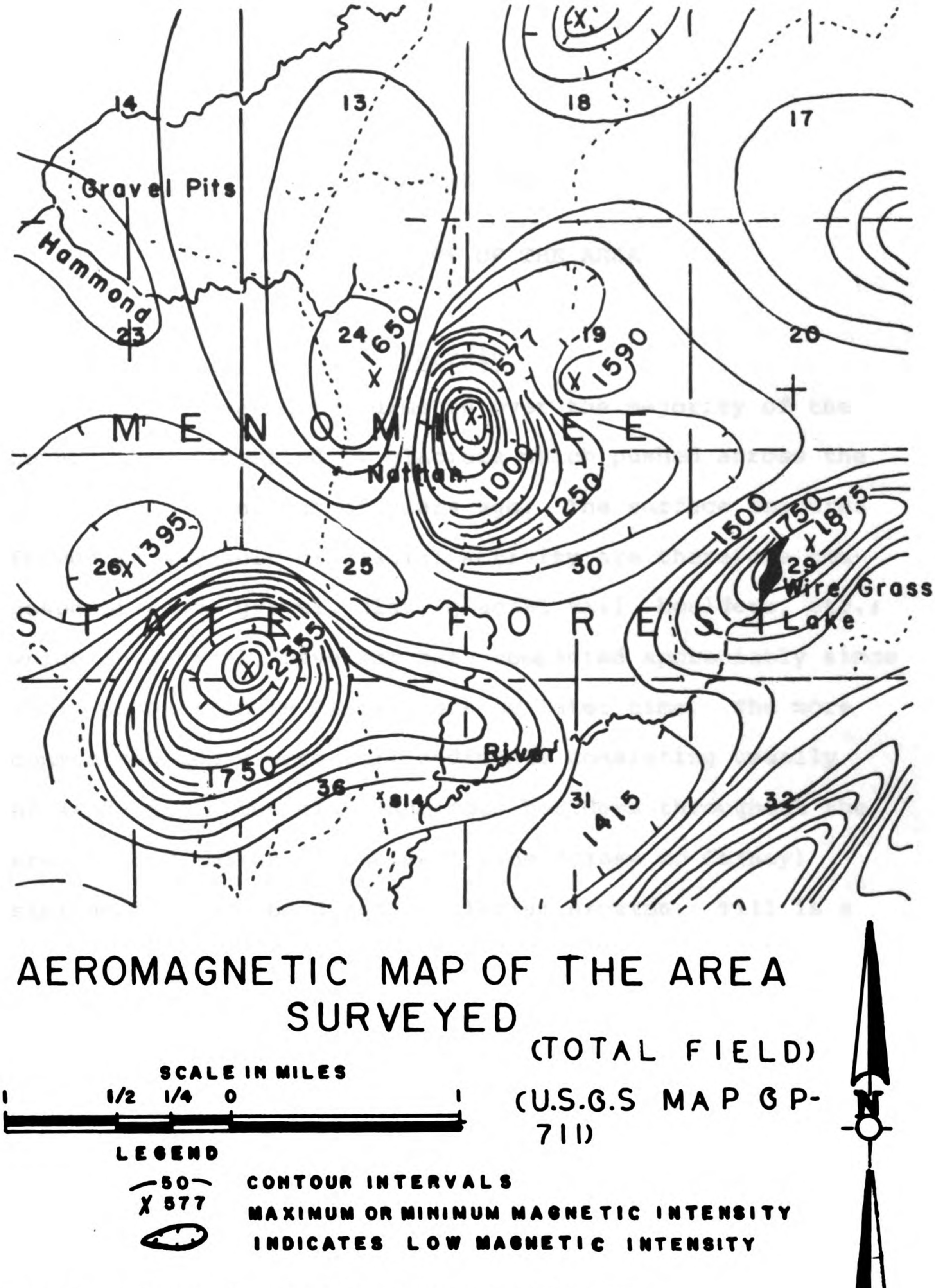

Fig. 4.--Total Intensity--Aeromagnetic Map.

CHAPTER III

GEOMORPHOLOGY OF THE AREA

Terrain

The uppermost sediments over the majority of the county were deposited by glaciers which pushed across the county many thousands of years ago. The surface features formed as a result of glacial activity are therefore composed of sand, gravel, clay, glacial till, boulders, etc.; which in general, have not been compacted appreciably since their deposition in Pleistocene or later time. The more common sediments were till sediments consisting usually of sandy and stony clay, numerous boulders throughout the area, and drumlins to the east side (close to Carney) similar to those produced by glacial erosion. Till is a mixture of sediments which have been deposited directly by the glacier (Vanlier, 1963). Generally, the moraines left by the glacier constitute approximately 50% of the area surveyed. The elevation of the moraines was variable between 802 feet and 892 feet. The maximum relief was 90 feet. Approximately 80% of the sixteen square mile quadrangle was covered by forest.

Low lands, between glacial deposits, developed marshy or boggy conditions due to the lack of adequate drainage. These boggy conditions stimulated growth of dense black spruce, tamarack and berry bushes. As one moved up and outwards from these areas of high water saturation, basswood, maple, and birch trees were common; intermingled with hemlock, Norway pine, and balsam firs that became more abundant as one went near the more cool, wind swept mounts of the glacial deposits. An area of particular interest was the boggy portion of the two northeast sections of the quadrangle. These sections were covered by extremely dense vegetation consisting of thorny berry bushes, small black spruce and tamarack. The density of these constituents was such that any attempt at traversing the area was prevented, rendering the gathering of data impossible. Since the primary determinant of vegetation is climatic condition with soil type being of secondary consideration any correlation of vegetation to bedrock would be a difficult task (especially when dealing with basement irregularities and glaciation).

CHAPTER IV

GENERAL GEOLOGY OF THE AREA

Though studied for nearly a century, the regional geology of the Upper Peninsula has not been completely defined primarily because of the covering of Paleozoic sediments and glacial drift. In view of this, several assumptions will be taken into account with the available geological data of the surrounding area.

The Menominee district (northwest of the area) is chiefly underlain by lower and middle Precambrian rocks, formerly designated Archean and Algonkian rock, which are covered extensively by Pleistocene glacial deposits, and locally by lower Paleozoic sandstone and dolomite. The lower Precambrian rocks occur in two separate areas, one in the northeast quarter composed of granitic gneiss (the Carney Lake Gneiss) and one in the southwest quarter composed chiefly of basaltic and felsic metavolcanic rocks (the Quinnesec greenstone) formation (Bayley, Dutton, and Lamey, 1966).

Lyons, Prinz, and Cain, quoted in William (1963) have investigated areas immediately north of the twelve-foot Falls Quartz Diorite. These writers agree that the

Newingham Granodiorite was emplaced by intrusion of a silicate melt, but their interpretation concerning other plutonic units differ markedly. Lyons concludes that this intrusion produced extensive metasomatism within the Quinnesec formation greenstones forming the Marinette Quartz-Diorite and Hosking Lake Granite in situ causing a strong local metasomatic effect. Prinz and Cain postulated a magmatic origin for all plutonic bodies of the area.

In the Menominee district (Bayley et al., 1966; Leith and Allen, 1915) found that the granite south of the Menominee River intrudes a series of basic volcanics called the Quinnesec schist which he correlated with the Keewatin. Although it was realized that the correlation of the Quinnesec schist as Keewatin introduced a conception of structure quite out of accord with natural inferences, it remained for Corey and Bowen (Leith and Allen, 1915) working under the direction of Van Hise and Leith in 1905 and Hotchkiss in 1910, to show conclusively that the Quinnesec schist is partly intrusive into, but in greater part interbedded with, the upper part of the Huronian (i.e., Animikie). Evidence of the present subsurface geology and structure has not been discovered or studied in Menominee County (Nathan area). Because of the veneer of glacial till in this area, subsurface geology will be correlated with well drillers records and outcrops that occur away from the surveyed area. Some of these drilling records will be described in Chapter IX, where they were used to draw a fence diagram in order to find an approximate depth to the top of basement rocks.

A general geology will also be inferred and assumed by reports that have been done by Dutton, Lamey, and Bayley (1966) and Russell (1906). Precambrian rocks form the bedrock in most of the Menominee district. They are overlain unconformably by Cambrian and Ordovician sandstone and dolomite in some areas, and all rocks are concealed in part by unconsolidated glacial deposits of Pleistocene age in most of the area. The rocks forming the Paleozoic system in the Menominee region include the Potsdam sandstone, the Calciferous cherty limestone and the Trenton limestone.

Chamberlin (1883) quoted in Russell (1906) described two great lobes of Pleistocene glaciation, the Green Bay lobe and the Chippewa lobe. The Green Bay lobe occupied the basin of Green Bay and extended southwest to the vicinity of Madison, Wisconsin and expanded westward. The Chippewa lobe expanded to the south now occupied by the western portion of the northern Peninsula of Michigan and adjacent portion of Wisconsin.

By an inspection of all measurements of drumlin trends and striations on bedrock, they served to show the general trend of ice motion which appeared to advance from

the northeast and as it moved over the land tended to change its direction (Nathan, Menominee County, secs. 26 and 35, 2-3 miles south of T38W; R28E). Dominant direction was N60E.

Although this particular area has not been examined in detail, enough is known concerning it to indicate that its covering of till is a part of the effects of the Green Bay lobe, and is possibly of the nature of an interlobate moraine. Naturally, these two great lobes mentioned and described by Chamberlin, must be correlated with the upward and subsidence movement described before by Russell.

CHAPTER V

GRAVITY FIELD SURVEY

Equipment

The instrument used in this study was a LaCoste-Romberg Geodetic Gravity meter (Figures 5 and 6). With a range of about 7000 milligals and a sensitivity of about 0.01 milligals. The meter has been designed to operate at a thermostated temperature of 48°C kept constant by a 12-volt battery or the eliminator (Figures 5 and 6). Compact rechargeable motorcycle batteries were used during this survey. Batteries were changed every night before the Gravity meter was to be used. The temperature of the instrument was controlled by its attachment to the battery eliminator/charger throughout the night. A concave base plate (Figures 5 and 6) was used. Extreme care was exercised to always reclamp the spring mechanism after three readings were taken for each station. The moving hairline was centered on the calibration-scale value of 2.60 and was always brought in from the right side of the scale to prevent hysteresis. It was necessary to turn the dial scale considerably to compensate for the change in latitude from East Lansing to Menominee County. Instrument drift

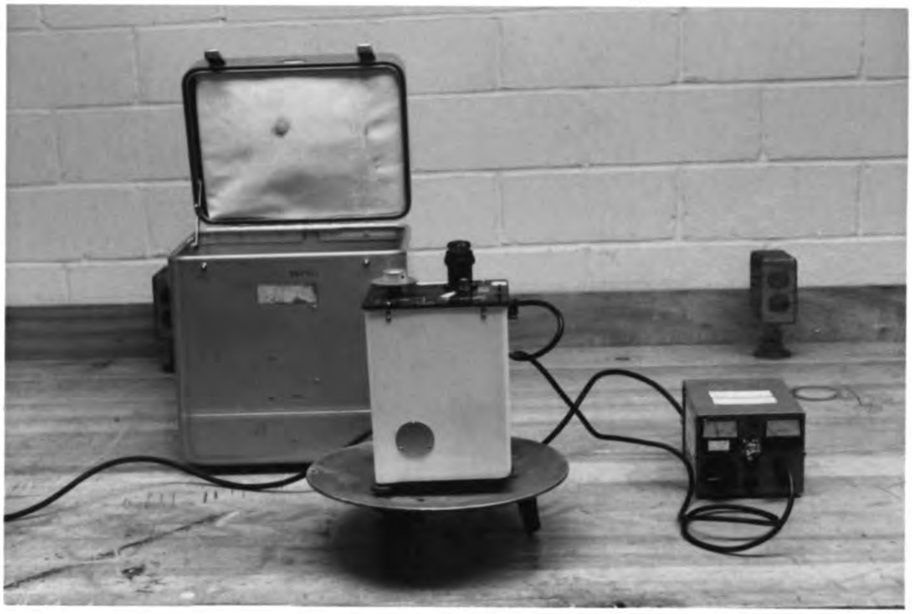

Fig. 5.--The LaCoste-Romberg meter, with the carrying case back, the concave base plate, and the eliminator charger connected to it.

Fig. 6.--A simulated reading, taken with the 12-volt battery attached to it.

Fig. 7.--From left to right, connection cable, battery charger, 12 volt battery, compass, and voltmeter.

(assumed linear with time) and earthtide effects were removed using correction curves (Figure 12) that were made by reoccupation of base station every 1-2 hours. Measurements between stations were either obtained by (1) car, (2) pacing, or (3) a sound producing object (in this case a car horn) which was in a known location.

Two Aneroid altimeters (the Wallace and Tiernan altimeter, the more sensitive and reliable extension of the aneroid barometer) were utilized during the survey to measure the elevation contrast of the gravity stations.

Description of and Determination of Altitude by the Wallace and Tiernan Altimeter

Within this instrument, changes in atmospheric pressure are exerted upon an evacuated beryllium copper capsule. Deflections of the capsule (caused by pressure variances) are transferred by a linkage to a geared sector which meshes with a pinion on the pointer shaft. The pointer is read on a dial that is calibrated in feet or in meters. Any lag in the reading is prevented by a device which eliminates backlash between the sector and the pointer pinion. A desiccant is enclosed in the instrument to absorb moisture that might otherwise collect and alter the readings. The instrument is mounted in a shockproof metal case and provided with an outer case and strap for carrying it in the field. An adjusting screw is provided in the face of the dial so that the instrument may be made to display a given bench mark elevation.

Due to the low temperature during the survey period, time consuming operation, and high fixed costs, both repetition of station altitude readings and continuous monitoring of base station deviation were not possible. This stipulation necessitated the method of determining elevation with one altimeter, a second one being utilized in order to check the reliability of the data.

The altimeter is taken to a starting point of known elevation, with the instrument adjusted to display the

Fig. 8.--A Wallace and Tiernan Altimeter. Zero on the scale equals -1000 feet, each small division is equivalent to 5 feet.

Fig. 9.--An altimeter showing the table of corrections inside of the instrument.

Fig. 10.--A second altimeter together with the last one was used in this survey also.

elevation of the base station (in this case, station number one, on the main road, corresponded to a bench mark, thereby providing an absolute measurement of altitude). The instrument is then taken to the various stations where an elevation is required, with the readings of time, altitude, and temperature being recorded. After a period of time, usually no more than two hours, the observer returns to the base station and records the aforementioned data again. Due to change in atmospheric conditions, the first and last readings at the base station will usually not agree. A correction must therefore be applied to the intermediate station readings. It is usually assumed that the change in the atmosphere has occurred uniformly with time. The

corrections are therefore computed in proportion to the elapsed time from the first observation. To obtain the correction factor, the base station deviance from absolute altitude (multiplied by a correction factor for temperature determined from a graph inside the altimeter) is compared to the time of day. This graph produces a curve within which intermediate stations may be plotted. The amount of deviation that corresponds to the station is either added or subtracted to the recorded altitude of that station. (The addition or subtraction of the deviant value is dependent upon the changing atmospheric pressure.) If a low pressure system is approaching, one measures an increase of base station readings. Correction factors would then be subtracted to adjust for the higher recorded elevations. The opposite would be performed, and addition, for the occurrence of a high pressure system.

The accuracy of altitude determination by this method was determined by analyzing the most deviant curve (as determined from a linear comparison of base stations). The graphs connecting the base stations were drawn from little data available for the exact determination of such curve (Figure 11).

Data points are represented by crosses and these are not meant to indicate error ranges.

The comparison of this linear representation of base station deviation (Figure 11) to the curved

GRAPH OF DEVIATION VS. TIME FOR ALTITUDE CORRECTION

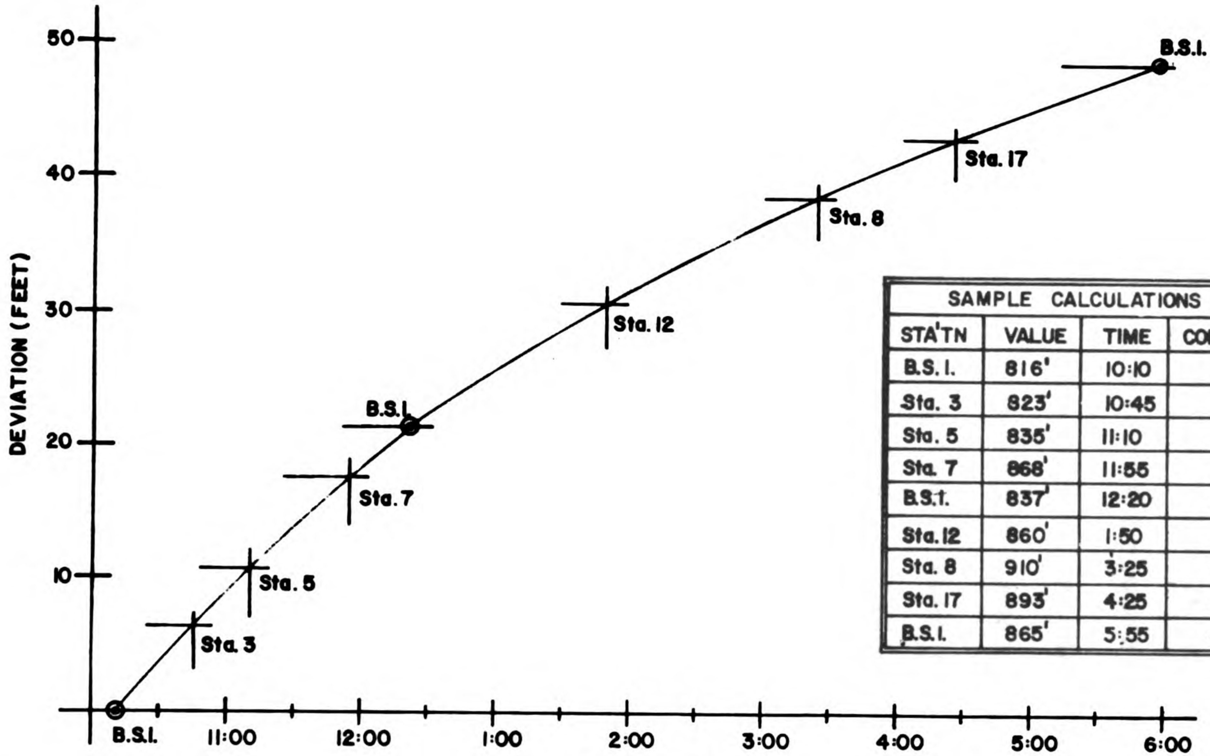

SAMPLE CALCULATIONS FROM 11-22-75				
STA'TN	VALUE	TIME	CORRECTION	ALTITUDE
B.S.I.	816'	10:10	0	816'
Sta. 3	823'	10:45	-6	817'
Sta. 5	835'	11:10	-11	824'
Sta. 7	868'	11:55	-18	850'
B.S.I.	837'	12:20	-21	816'
Sta. 12	860'	1:50	-31	829'
Sta. 8	910'	3:25	-38	872'
Sta. 17	893'	4:25	-43	850'
B.S.I.	865'	5:55	-49	816'

FIGURE 11

NOTE:
DEVIATION OF 49' WAS OBTAINED FROM MULTIPLING THE ABSOLUTE DEVIATION (50') BY AN INSTRUMENT CORRECTION FACTOR (.98), FOR THE 40° f. TEMPERATURE.

representation produced an error of an absolute two feet. This error combined with instrument error (accuracy to approximately two feet) produce a maximum deviation of approximately .37 mgals. The accuracy of time measurements was to several minutes, this deviation being negligible.

Because of the deflection effects of the anomalies on a magnetic compass, measurements between stations were either obtained by pacing or by time consumed between known points along the main road. Stations along the main road and some medium duty roads were taken with a car. Light duty roads and unimproved dirt roads (Figure 1-1, topographic map) were very useful to obtain most of the swamp gravity and magnetic station (Figures 2 and 3).

Survey Sampling Area

The first step done was to set up a grid pattern (rectangular coordinate system) for staking. Staking is an important basic operation and should be carried out accurately. These series of points, at which the geophysical measurements were made, were marked off at an interval of 1/8, 1/4 and 1/2 miles in a four square mile coordinate system (Figures 2 and 3). Since one side of the square could have 17 stakes, the total number necessary, throughout the regular staking network, would be 17 x 17 or 289 stations. As time, weather conditions, terrain irregularities, and survey expense allowed, it was only possible to reach approximately 152 staking points to obtain gravimeter readings. Each stake was colored, with spray point, a bright orange or reddish color so as to help us reoccupy exactly the same observation stations for magnetic readings, which at times were made concurrently with the gravity readings. The purpose of staking is to establish a coordinate system in which every observation station is clearly and uniquely marked, allowing any follow-up work to be directed to the proper places.

Secondly, since more than one geophysical method was used, staking helped to reoccupy exactly the same stations so that a comparison of the results of the various methods is rendered reliable. The first group of stakes along the main medium duty road (this was chosen to be a straight road, which fortunately, ran directly East-West cutting our coordinate system exactly in half (Figure 1-1 and 2) served as the first traverse for elevation, markings, and gravimeter readings and also for future magnetic readings. It was from this base line that all subsequent readings were taken--a series of parallel lines perpendicular to and parallel to the base line at intervals described on the page before. The single most important thing in staking the area was the use of the topographic map (Powers Quadrangle, Michigan, 15 minute series, Mapped, Edited, and Published by the U.S. Geological Survey). From this it was possible to locate the points for the regular interval of .25 miles from the topographic features the edge of a wooded area next to a clearing, hills, valleys, swamps, etc. The method of pacing was very useful in plain areas, although it became too cumbersome for extended distances while climbing over hills and working our way through the forest and swamps. The topographic map was also indispensable to correlate with the altimeter elevation survey. In addition, some topographic detail was recorded at each observation station (i.e., location of relationship to fences, houses, hills, etc.).

In the Nathan anomaly area a uniform grid spacing was used where it was possible although 80% of the area was covered by swamp and heavily forested. Proper orientation in the woods was sometimes difficult because of the magnetic disturbances. Frequently the sun was used for a proper fix on our location.

Low gravity values were observed close to the area. These low values of gravity can be seen on the Bouguer gravity map at both sides (East-West) of the higher positive anomaly. These changes were smoothed on the Bouguer gravity map, and the regional effect was estimated in accord with possible lithologic changes (less dense sediments) which could be the main reason of this natural effect.

Measurement Method

Once our rectangular area (4 x 4 miles) was chosen, a well-defined convenient point in the area, for a straight base line was determined. This was a straight medium duty road which divides our coordinate system exactly in half (Figure 1-1 and 2). The gravity survey consisted of establishing a grid of perpendicular lines to gain an approximation to the area size of the anomalies and to establish a grid pattern throughout the regular staking network, providing a base station pattern for future use. Three gravity reading were taken for each station, with the average value calculated, and the time and elevation data simultaneously recorded. Reoccupation of base station was done every 1-2 hours to correct for drift and diurnal effects. At the beginning of this survey, when most of the readings along the medium, light, and unimproved roads were taken, only one base station was necessary to use. Naturally, all of these readings were taken with the car which helped the crew return to the base station at least every two hours.

The base station altimeter was always located at bench marks, main medium duty road (where the elevation is known with the help of Powers Quadrangle topographic map, Figure 1-1), or with a gravity station, where the elevation had been previously determined. The maximum error combined with instrument error was plus or minus 4 feet. A reference point (station number one) far from artificial disturbance such as those due to railways, constant traffic way, swamps etc. was chosen and the gravity intensity values at all other points were measured as positive or negative differences from the intensity at this point. The reference point may, strictly speaking, be anywhere within or without the area, but it is convenient to choose a point, as near as possible to the area or inside it, at which the gravity field is known to be approximately the normal field.

CHAPTER VI

CORRECTIONS TO GRAVITY OBSERVATIONS TO YIELD THE BOUGUER GRAVITY RESIDUAL

Instrument and Diurnal Corrections

When the gravity values in the form of milligals, a correction may be employed to compensate the values for fluctuations caused by instrument and diurnal variations. Instrument variation is due to the creep in the spring mechanism of the gravimeter. The quartz spring gradually stretches due to the load imposed upon it by gravity. This stretching manifests itself in the base station readings, by indicating an overall apparent increase in gravity as the reading continues to be taken. Diurnal (or tidal) variations occur with twice daily cycles as a result of changes in the moon's and sun's position relative to a fixed point. These extraneous bodies have an effect on the earth's crust much the same as they have on water. The amount of gravitational attraction in tidal sequences produces a change in gravity readings that may be predicted by a curve. Since these sources of error, instrument and diurnal, are inherent and concurrent, they may be analyzed and corrected for simultaneously; thereby giving one a more accurate assessment of the anomalous mass.

The method chosen for performing this correction involved the reoccupation of the base station at intervals of 1-2 hours and the reading of the gravimeter. If it was not feasible to return to the base station, another nearby station (whose relation to the base station had been previously recorded) was monitored, throughout the day, it was related to the first base station by incorporating its deviation into the first base station's deviation at the time the secondary base station was first read. Once this had been accomplished, a smooth curve was drawn through, or as near as possible, the points (Figure 12). From this curve, one obtains the readings that the gravimeter would have displayed had it been at the base station continuously. The value of the curve at the time a station was recorded, gives one the value to be added or subtracted to that reading. (A value is added if the base station readings decrease throughout the day, and subtracted if the base station readings increase throughout the day).

In this survey, the maximum deviation on a given day, due to instrument and diurnal effects, was .2 milligals. Most generally, this deviation did not exceed .1 milligal. Upon fitting various smooth curves to the data points, it was found that an error of approximately 8% of the total deviation could be incurred. This correction

GRAPH OF DEVIATION VS. TIME
FOR CORRECTION OF GRAVITY INSTRUMENT AND DIURNAL VARIATIONS

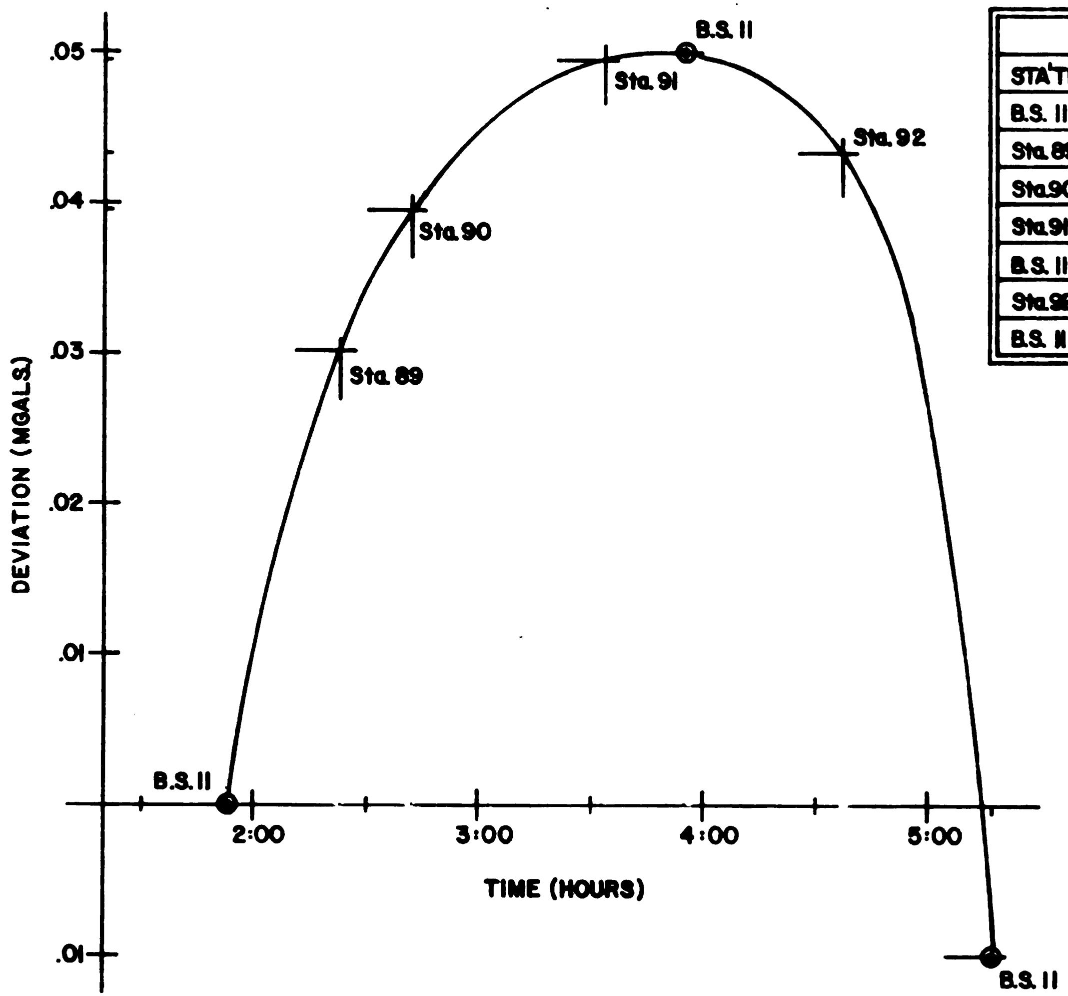

SAMPLE CALCULATIONS FROM 12-15-75				
STA'TN	VALUE *	TIME	CORRECTION	TRUE VALUE
B.S. 11	4400.05	1:55	0	4400.05 mgls
Sta. 89	4400.86	2:23	-.03	4400.83 "
Sta. 90	4401.23	2:42	-.04	4401.19 "
Sta. 91	4399.12	3:33	-.05	4399.08 "
B.S. 11	4400.10	3:55	-.05	4400.05 "
Sta. 92	4400.34	4:37	-.04	4400.30 "
B.S. 11	4400.04	5:17	+.01	4400.05 "

* ALL VALUES HAVE BEEN CORRECTED TO BASE STATION NO. 1

FIGURE 12

corresponds to a maximum deviation of .016 milligals from a corrected reading. This correction was made by a calculator machine as were the corrections for Free-Air and Bouguer, elevation, and latitude. Also, here, data points are represented by crosses. They are not meant to indicate error ranges.

Free Air and Bouguer Corrections

An elevation correction was made to take account of the fact that gravity changes with elevation, because a higher station is farther away from the center of the earth than a lower one and gravity is affected by the attraction of material under the station. The correction has two components: (a) The Free-Air, which is due to the vertical gradient of gravity. The magnitude of this effect is 0.09406 mgal/ft and it was added to the observed gravity values. This magnitude was obtained subtracting the gravity difference between sea level and a point of elevation "h" (Dobrin, 1960).

$$Go - \frac{R^2}{(R + h)^2} Go = Go \left(1 - \frac{R^2}{(R + h)^2}\right)$$

where: Go = Gravity value at sea level

R = Mean radius of Earth

Since h is much smaller than R,

$$\text{Change in gravity} = \text{(approximately)} \; \frac{2\,Goh}{R} =$$

$$0.09406 \text{ milligal/ft}$$

(b) The Bouguer Correction, which accounts for the attraction of the rock material between sea level and the stations. The attraction in milligals of an infinite slab of thickness h (ft) is $2\pi\gamma\sigma h$ (Dobrin, 1960), where σ is the assumed average density for crustal rocks, and γ is the universal gravitational constant (6.670×10^{-8} dyne-cm^2/gm^2).

It was necessary to assume an average density value for these rocks. This average density is about 2.6 gm/cm^3 (Anderson, 1974), so the Bouguer correction was .033 milligals per foot and it was subtracted from the observed gravity. The combined Free-Air and Bougher correction was .061 milligals per foot and its error was calculated at plus or minus .10 milligals.

Latitude Correction

The international gravity formula for the variation of normal gravity along the geoid with the latitude $\emptyset$ is:

$$G = 978.049\ (1 + 0.0052884 \sin^2 \emptyset - 0.0000059 \sin^2 2\emptyset)\ \text{gal}$$

where: 978.049 = value of gravity at the Equator.

It is seen that the gravity at the equator ($\emptyset = 0°$) is about 5,000 milligals less than at the poles ($\emptyset = 90°$). The rate of change of gravity along a north-south line is obtained by differentiation of the equation above mentioned, and it is:

$W = 1.307 \sin 2\phi$ milligals per mile

In the Nathan anomaly area the latitude value is approximately 45.58°, thus W = .33 mgals, for the change for every 1/4 mile (approximately 1,320 feet) and was added for stations to the south of the main medium duty road (base line), and subtracted for stations to the north of the same road. Latitude distances were mapped and measured with the help of a grid pattern (4 x 4 miles, each 1/4 mile) and a topographic map of the area with a maximum error of 100 feet causing a gravity error less than plus or minus 0.03 milligals.

The Bouguer Gravity Map and Removal of Regional Effects

After the application of all corrections already mentioned, a Bouguer gravity map was constructed. This is the ordinary "observed" gravity map on which the primary results of a gravity survey are presented (Figure 2-1). The gravity stations (Figure 2) plotted on a grid pattern, with (4 x 4 miles), was used to contour the gravity readings. It was so regular that this simple method can give accurate enough results for exploration work. The contour interval was chosen to be .5 milligals and the scale was in miles.

Regional Effects

To bring out the local anomalies in relief, the regional effects were removed by graphical smoothing as illustrated in Figure 12-1. This gravity cross section was drawn through both centers of the main anomalies. After several other calculations, it was shown to be the best gravity cross section to represent the closer symmetrical pattern. This regional effect was sketched by the regular method of smoothing. On subtracting it from the observed curve, the local anomalies were obtained. Regional gravity lines were connected across the interval of the anomalies on each profile with the provision that the difference of regional and anomalous gravity at each point on the profile, corresponded to a perpendicular profile (Anderson, 1974). One of these profiles, together with others, were necessarily drawn along a North-East, South-West direction (Figure 2-1) to obtain the best gravity cross-section under the provisions already mentioned. This procedure could also be used to remove the effects of two nearby low gravity anomalies on both sides of the Bouguer gravity anomaly (3.77 mgals, Figure 2-1). However, because of the practically unknown geology and the impossibility of establishing a constant regional pattern, the decision was to draw the best gravity cross-section where the closer symmetrical pattern could be estimated. Discussion about nearby anomalies will be done in a later chapter (Gravity Interpretation).

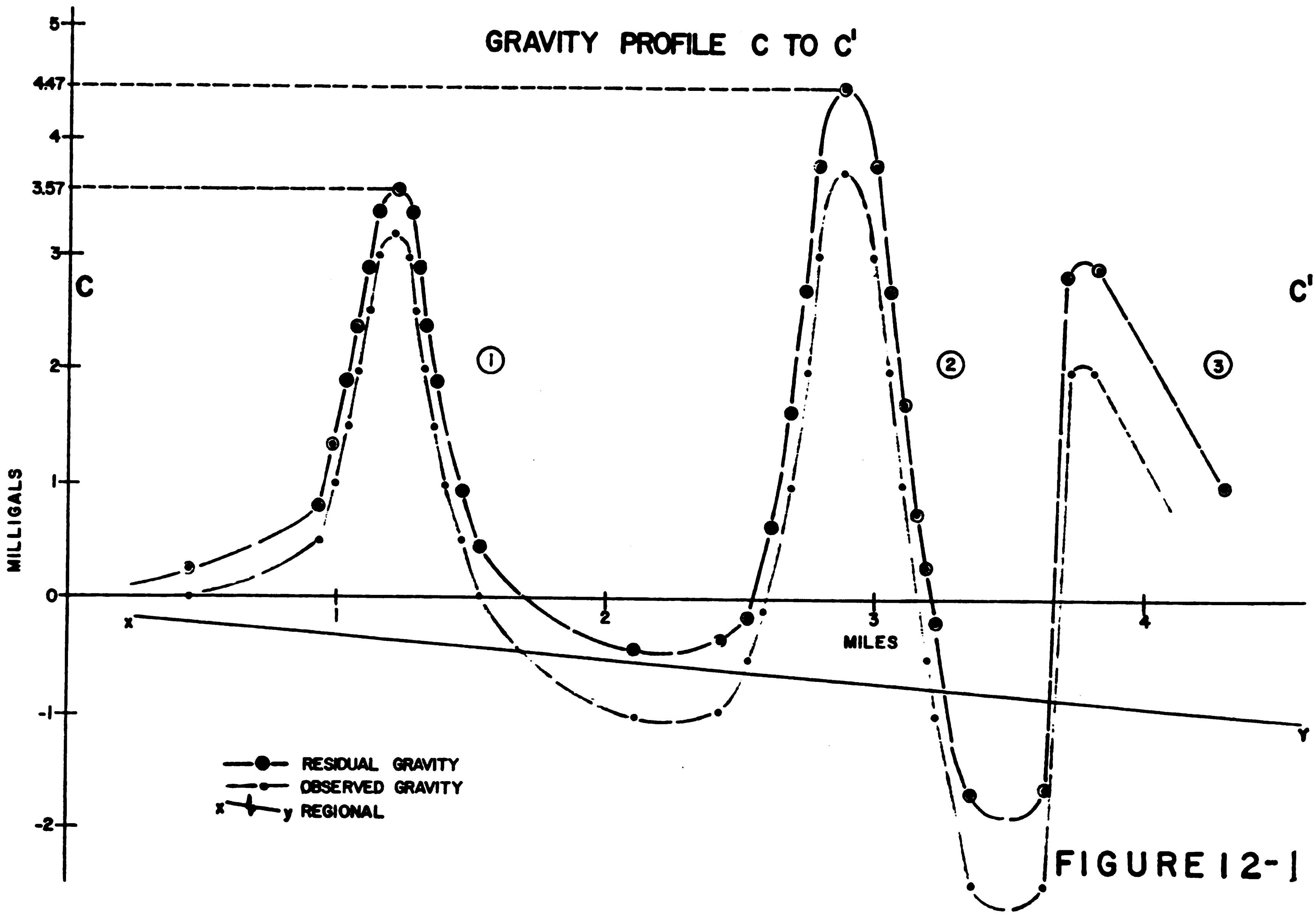
GRAVITY PROFILE C TO C'
MILLIGALS
5
4.47
4
3.57
3
2
1
0
-1
-2
C
C'
1
2
3
4
MILES
x
Y
RESIDUAL GRAVITY
OBSERVED GRAVITY
x y REGIONAL

FIGURE 12-1

Estimation of Maximum Gravity Error

The reading of the gravity meter is sensitive to about .01 milligal. The error in elevation was a maximum of 4 feet combined with instrument error; corresponding to a maximum deviation of approximately .37 milligals. Mapped station locations were accurate to within 100 feet, causing a gravity error of plus or minus 0.03 milligals. The total maximum error was 0.40 milligals, not inclusive of terrain errors that arise mainly from the error in elevation determination.

CHAPTER VII

MAGNETIC FIELD SURVEY

Equipment

Magnetic stations were read using a Flux-Gate Magnetometer (Scintrex, Model MF-2-100). With its internal sensor, it measures the vertical component of magnetic field intensity. The full-scale meter ranges are 100 gammas (resolution ± .5 gammas), and 300, 1000, 3000, 10000 (10K), 30000 (30K), and 100,000 (100K). Resolution is ± .5% of full scale on each range. In our case, for the northern hemisphere, the range is set for +80,000 to -20,000 gammas. Temperature stability is 1 gamma per °C. A battery pack was required (16 C-cell, 1.5 volt, alkaline batteries) for this survey, and it was not necessary to use more than one set in order to complete the area surveyed. It was necessary to turn the meter scale several times in order to set the scale at some range which would be slightly larger than the maximum gammas exhibited by the airborne survey. The aeromagnetic map published in 1970 by the U.S. Geological Survey (Map GP-711) provided the aeromagnetic contour lines of high and low values which were used in the first instance to test and see if

Fig. 12-2.--Flux-Gate Magnetometer showing the main switch off. Battery cable attached on instrument's base.

Fig. 12-3.--Flux-Gate Magnetometer showing the "+" position (positive, for vertical field directed downward).

the readings were of an appropriate value, such that they would not necessitate the continual changing of scale. As in gravity, a base station was reoccupied every 1-2 hours to correct for diurnal variation, any instrumental drift, and temperature coefficient.

Survey Sampling Area

Certain precautions were taken in carrying out all magnetic field work. All metallic objects were removed from our wearing apparel (i.e., wristwatch, keys, penknife, etc.). Other objects often avoided were steel wires in spectacle frames, power lines, pipe lines, nails in field shoes, etc. The grid pattern (rectangular coordinate system) used for gravity readings, was used for magnetic readings also. Stakes at these stations were colored with spray paint and reoccupied at various times. It was possible to reach only 133 staking points of the gravity grid pattern to obtain magnetic readings. A tripod for fixing the magnetometer naturally was used several times, and an error of ± 5 gammas was observed. The Flux-Gate magnetometer was used most of the time by attaching the carrying strap to the instrument and using the upper buttons to maintain the same height at the same location for more accuracy in the control of daily (diurnal) variation of the Earth's magnetic field.

Fig. 12-4.--Flux-Gate magnetometer, battery pack (16 C-cell, 1.5 volt) and tripod are attached to the instrument.

The Zero Level

One of the most important points in considering the magnetic anomalies in the area was the zero level. (The reading of the magnetometer at points where there are not appreciable disturbances from subsurface masses so that only the "normal" geomagnetic field is present.) It is often difficult to decide about a suitable zero level, however with the aeromagnetic survey flown and compiled by the U.S. and Michigan Geological Surveys (flown at 500 feet above ground, 1966), it was possible to choose a suitable beginning "working zero." All readings were corrected at the end of the survey by adding to or

subtracting from them, a constant amount arrived at from the study of the resulting anomalies. The suitable "working zero" was chosen at base station number one, along the main medium duty road where disturbance from subsurface masses was negligible.

CHAPTER VIII

REDUCTION OF MAGNETIC DATA TO YIELD THE VERTICAL INTENSITY GROUND MAGNETIC MAP

Before magnetic readings can be mapped, several corrections must be applied. These are the diurnal correction, the temperature correction, the normal correction, and the terrain correction (under special conditions).

Correction of Magnetic Values for Instrument and Diurnal Variations

In this survey, the values obtained from the magnetometer were corrected for variations caused by instrument and diurnal effects. Diurnal variations are those initiated by the sun's emission of high energy particles and effect on the ionosphere, and the moon's gravitational effect upon the ionosphere. They constitute the predominant effect upon reading deviation. Instrument variation originates from any inability of the magnetometer to reproduce a reading. Because of this, mitigating factors such as leveling and temperature have an effect on instrument variation.

The procedure utilized in this survey that allowed for the correction of these variations involved the repetition of readings at a base station (or any previously occupied station whose relation to the base station was known) at intervals of 1-2 hours. The base station deviations (and deviation of other stations if used) were plotted on a graph against time (see curve sample, Figure 13). In cases where more than one base station was monitored on a given day, it was related to the first base station by incorporating its deviation into the base station deviation at the time the secondary station was first read. Once this had been accomplished, a smooth curve was drawn through (or as near as possible to) the points. If the repeated readings showed an increase, the amount of increase was subtracted from that intermediate station's value at the time the station was read. If the repeated readings exhibited a decrease, the amount of decrease at the time an intermediate station was read, and was added to that station's value.

During the survey, negative and positive values over the anomalous bodies were recorded. To more easily facilitate the correction of these readings, a suitable zero level station was arbitrarily chosen; all values greater, being positive, and lower, being negative. After the corrections were completed, the values were once more assigned their respective positions in exhibiting

GRAPH OF DEVIATION VS. TIME
FOR CORRECTION OF MAGNETIC INSTRUMENT AND DIURNAL VARIATIONS

SAMPLE CALCULATIONS FROM 1-24-76				
STA'TN	VALUE	TIME	CORRECTION	TRUE VALUE
B.S. I	0	11:45	0	0 gammas
Sta. 109	+2	12:30	+28	+30 "
B.S. 112	+31	12:56	+42	+73 "
B.S. I	-50	1:10	+50	0 "
B.S. 112	+17	1:40	+56	+73 "
Sta. 114	-39	2:10	+61	+22 "
B.S. 112	+7	3:00	+66	+73 "
B.S. 112	-2	4:35	+75	+73 "
B.S. 1	-100	5:00	· +100	0 "

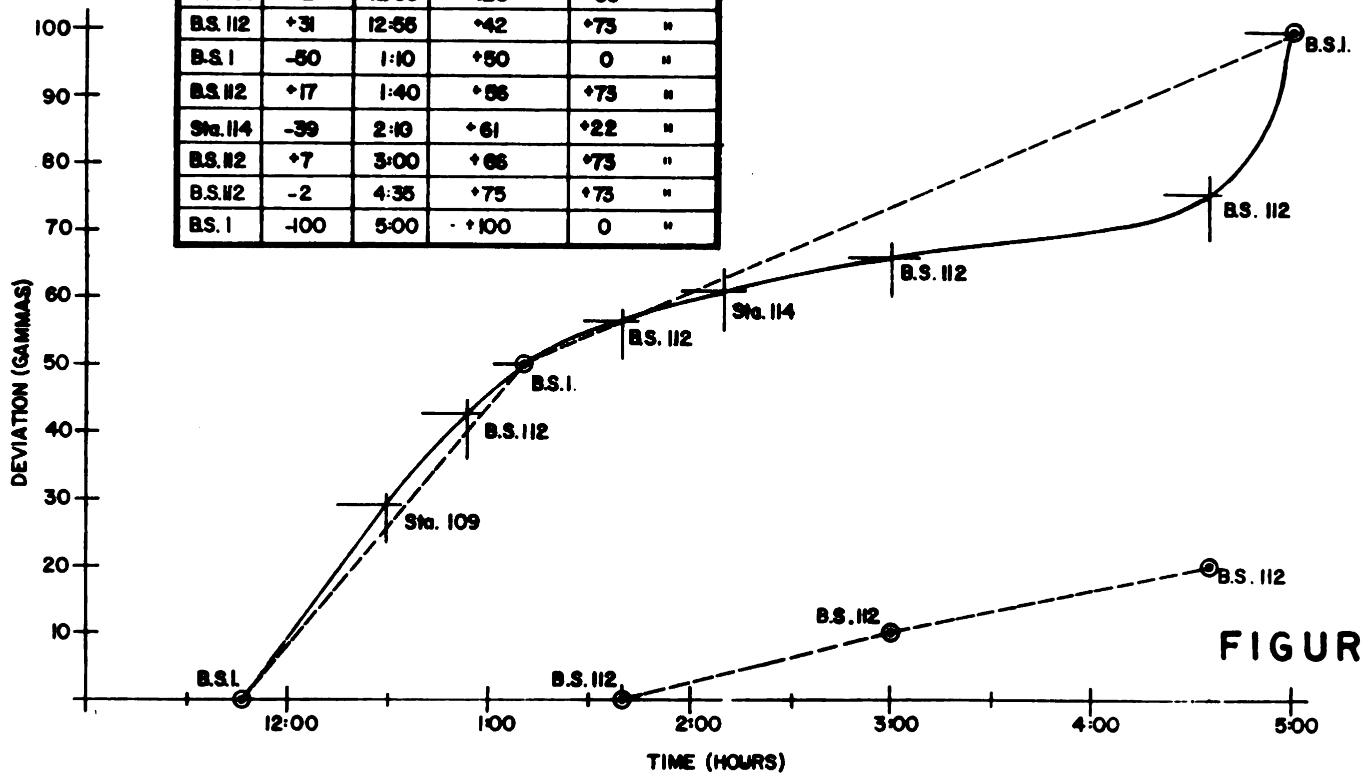

FIGURE 13

the polarity of the anomalous mass. The maximum deviation due to instrument and diurnal variations on a given day was found to be 520 gammas. These values were discarded as being due to a magnetic storm; value displayed for those stations coming from readings of a later expedition. The deviation of utilized days was approximately 60 gammas. Upon fitting of various smooth curves through the data points, an error of approximately 12% could be apparent. This corresponds to a maximum deviation of approximately 15 gammas from a corrected reading.

In this survey, a compensated magnetometer was used and a temperature coefficient was included together with the drift in the diurnal variation correction thus the temperature correction was not necessary.

Normal Corrections

Throughout historical time, continual changes in the magnitude and direction of the earth's main or "permanent" field has occurred as one moves about the surface of the earth. These changes correspond in a sense, to the variations of the earth's gravity with latitude. However, normal magnetic changes over the earth are not regular functions of latitude, as is the case with gravitational field. This variation, which cannot generally be correlated with known geologic features, is in many cases similar to the large scale regional variations often observed in gravity work. Where the survey was confined to a small area of sixteen square miles, and where the geologic structure are unknown and possibly of large horizontal scale, this reduction was neglected.

Terrain corrections were also neglected because there was not an appreciative difference in elevation capable of necessitating such a correction. In general this area can be considered flat, which means that a correction of such magnitude will not affect our readings appreciably.

CHAPTER IX

FENCE DIAGRAM OF MID-MENOMINEE WELLS AND ITS INTERPRETATION

Since there is an absence of "upper limestone" and "middle limestone and sandstone" to the north of the quadrangle surveyed (Fig. 14-1, Fence Diagram), one could expect a somewhat similar lithology within the quadrangle. As the "Fence Diagram" exhibits, there is a transition from glacial drift to the lower sandstone which rests upon the Precambrian rocks. From figures (N° 14, 14-1), one notices that the stratigraphy dips towards the southeast in the same direction as the occurrence of thickening beds. The fence diagram was constructed with six logs of wells (the closest to the area surveyed) and their description is as follows: Well N° 1 (38N 26W 16-1), Well N° 2 (35N 27W 23-3), Well N° 3 (37N 28W 11-1), Well N° 4 (35N 28W 19-1), Well N° 5 (35N 25W 35-1), and Well N° 6 (38N 28W 9-1) (Vanlier, 1963). At well N° 6, approximately 9 miles to the northwest, the Precambrian rests directly beneath the glacial drift at a depth of 19 feet. At well N° 4 approximately 10 miles to the southwest, the Precambrian resides at 162 feet below the surface. This

SCHEMATIC BLOCK DIAGRAM OF MID-MENOMINEE COUNTY

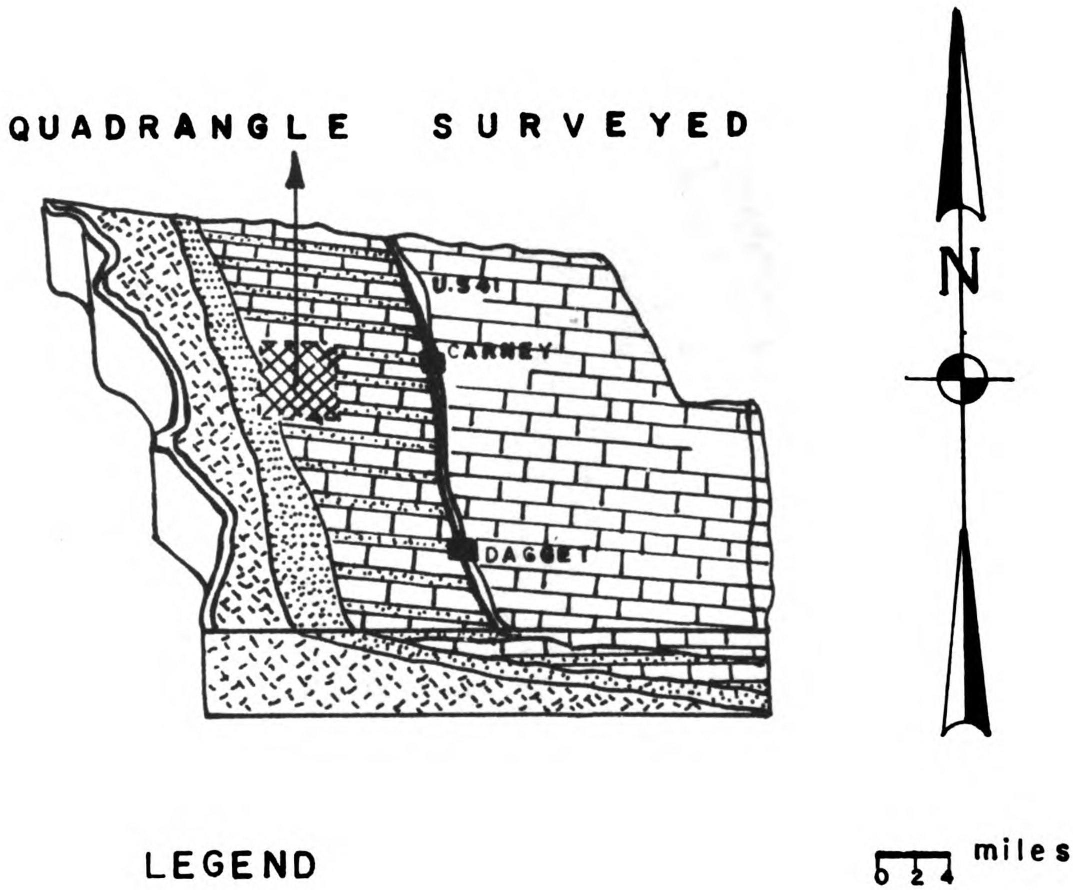

LEGEND

UPPER LIMESTONES

MIDDLE LIMESTONES AND SANDSTONES

LOWER SANDSTONE

PRECAMBRIAN ROCKS

FIGURE. 14

FENCE-DIAGRAM OF MID-MENOMINEE WELLS

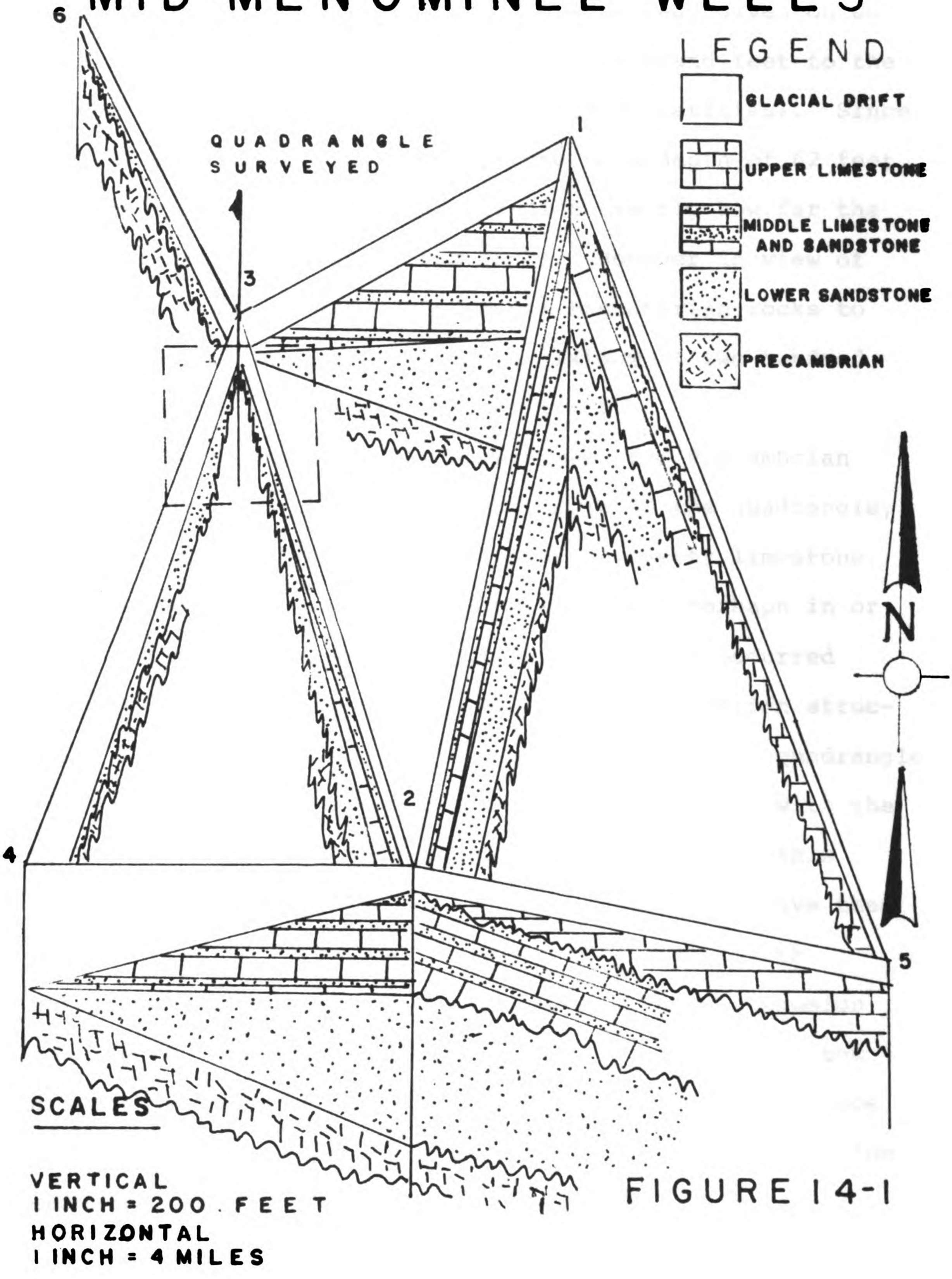

FIGURE 14-1

indicates a gradual inclination of the basement rocks, that when extrapolated to the quadrangle surveyed, gives on an approximate depth no greater than one thousand feet to the top of the Precambrian (assuming no irregularities). Since well N° 3 obtained a lower sandstone to a depth of 62 feet and was abandoned, one cannot predict exactly how far the drilling was from Precambrian rocks. However in view of the fence diagram, one could expect Precambrian rocks to lie at a depth of not more than a maximum of two hundred feet below the quadrangle (Figure 14-1).

To the south of the quadrangle, the Precambrian rocks consist of granite. To the north of the quadrangle, one finds the Precambrian to consist of cherty limestone. This irregularity leads one to believe that perhaps in or near the area of the quadrangle, an event has occurred which has resulted from a change in the Precambrian structure. Perhaps a fault running east-west near the quadrangle and parallel to the Menominee range to the north, with the rock to the north being the graben, might explain this feature. The graben and horst assemblages could have then been covered by a Precambrian sea, resulting in both being covered by limestone. As time progressed, erosion down to the previous basement granite of the horst block did not wear through to the granite of the graben. Since the graben was filled with limestone, limestone was at the same erosional level as the granite to the south of the

quadrangle. At this time, the postcambrian sea and current resulting stratigraphy were developed. The anomalies in the quadrangle could be due to the intrusion of ferro-magnesian dikes, resulting from the deformational process surrounding the fault.

CHAPTER X

GRAVITY INTERPRETATION

Approximation by a Cylinder

In this chapter an attempt has been made to interpret positive gravity anomalies due to causes such as rock masses emplaced in rocks of higher density, sediments with density lower than that of the surrounding rocks, or any other process which can account for a density contrast between rocks of different sources. In order to determine the parameters of the anomalous masses it was necessary to fit a regional trend, which when subtracted from the Bouguer anomaly, would yield the residual anomaly of the mass. The best regional value (on a profile North-East, South-West, Figure 2-1) was fitted graphically taking advantage of the good anomaly boundaries on this profile.

The interpretation procedure was to treat the anomalous masses in the basement as vertical cylinders, because of the concentric symmetries of the geophysical anomalies. Two approximation techniques were used; the vertical line element or axial line element, and solid angles.

Vertical Cylinder Approximation by Axial Line Element and Solid Angles

An important class of geologic structure that is more or less vertical is intrusive igneous plugs. These are often represented for the purpose of analysis by vertical right cylinders. Unfortunately, calculating the gravity effect of a vertical cylinder is easy only on the axis. At all other points the calculation is difficult, involving elliptic integrals or series expansion of Legendre polynomials. Therefore, approximation to the gravity effect of vertical cylinders are important in practice (Hammer, 1974).

Approximation was done by a vertical cylinder to best fit the observed radial profile values of gravity at various depths and radius. A minimum density contrast of .30 to a maximum of .45 grams per cubic centimeter was necessary because of the higher density of iron-rich formation possibly present there (Bacon, unpublished report).

The formula used for calculating gravity over a finite vertical right cylinder is:

$$\Delta gz = 6.39\ R^2 \Delta\sigma \left[\frac{1}{Z_1\ (1 + X^2/Z_1{}^2)^{1/2}} - \frac{1}{Z_2\ (1 + X^2/Z_2{}^2)^{1/2}} \right] \quad (1)$$

where: Δgz = vertical gravity anomaly (milligals)

R = radius (Kilofeet)

$\Delta\sigma$ = density contrast (gm/cm^3)

Z_1 = depth to the top of the cylinder (Kilofeet)

Z_2 = depth to the bottom of the cylinder (Kilofeet)

X = horizontal distance from the center (Kilofeet)

Vertical Line Element Formula

The above expression was used for cylinders of finite length (top at depth Z_1, bottom at depth Z_2) by simply subtracting the effect calculated for depth Z_2 from that calculated for depth Z_1. All distances are expressed in Kilofeet (convention for numerical constant) and the vertical gravity (Δgz) in milligals (Nettleton, 1942; Hammer, 1974).

For solid angles:

(2) $gz = 2.03\ W\Delta\sigma t$

where: gz = vertical gravity anomaly (milligals)

$\Delta\sigma$ = density contrast (gm/cm^3)

t = thickness (i.e., $Z_2 - Z_1$)

The thickness or length (i.e., $Z_2 - Z_1$) of each cylinder must be less than or equal about half its mean depth, so its gravity effect can be approximated closely enough for most geophysical purposes by considering the mass to be condensed upon its median plain and calculating the effect in terms of the solid angle subtended by the boundary on the plane. Values of "W" can be read from the solid angle chart (Nettleton, 1942; 1971), from the ratio Z/R (which is constant for any given case) and the ratio X/Z.

Calculation of solid angles for even simple boundaries is mathematically difficult and tedious but they can be calculated for circles. This is useful for calculating gravity effects for any body which can be approximated by horizontal circular slabs. The calculated profiles of gravity over the cylinders (by the vertical line and the solid angles method) were compared to the residual gravity anomalies (Figures 16 and 16-1). The cylinder that best fitted the positive gravity anomaly (3.57 milligals) southwest of the area surveyed had a radius of .8 Kilofeet (Figure 16). This close fit of calculated and actual gravity was possible applying the solid angle method, with a density contrast of .45 gm/cm^3 (the maximum utilized) and calculating the sum of the solid angles (Hammer, 1974) of 8 thin circular slices to achieve an error on the axis no greater than -6%. Axial errors (expressed as a percentage of the central anomaly magnitude for the cylinder) for a family of vertical cylinders are shown in Figure 17 (Hammer, 1974). This close fit of calculated and actual gravity permits the calculation of an approximated value for the volume of the cylindrical model. This volume was determined by the formula:

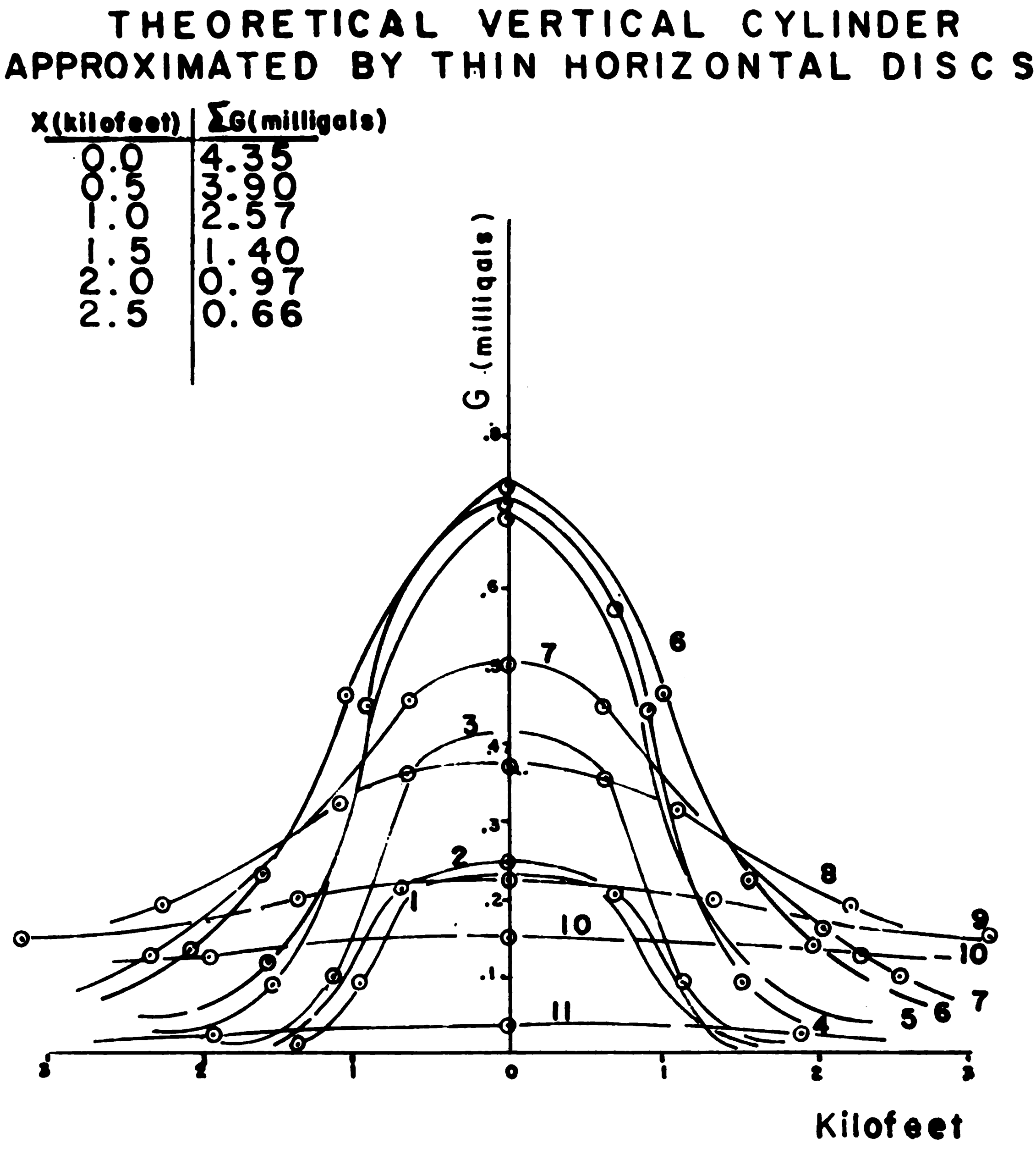

Fig. 15.--Theoretical Vertical Cylinder Approximated by Thin Horizontal Disc.

VERTICAL GRAVITY PROFILES OVER CYLINDRICAL MODELS

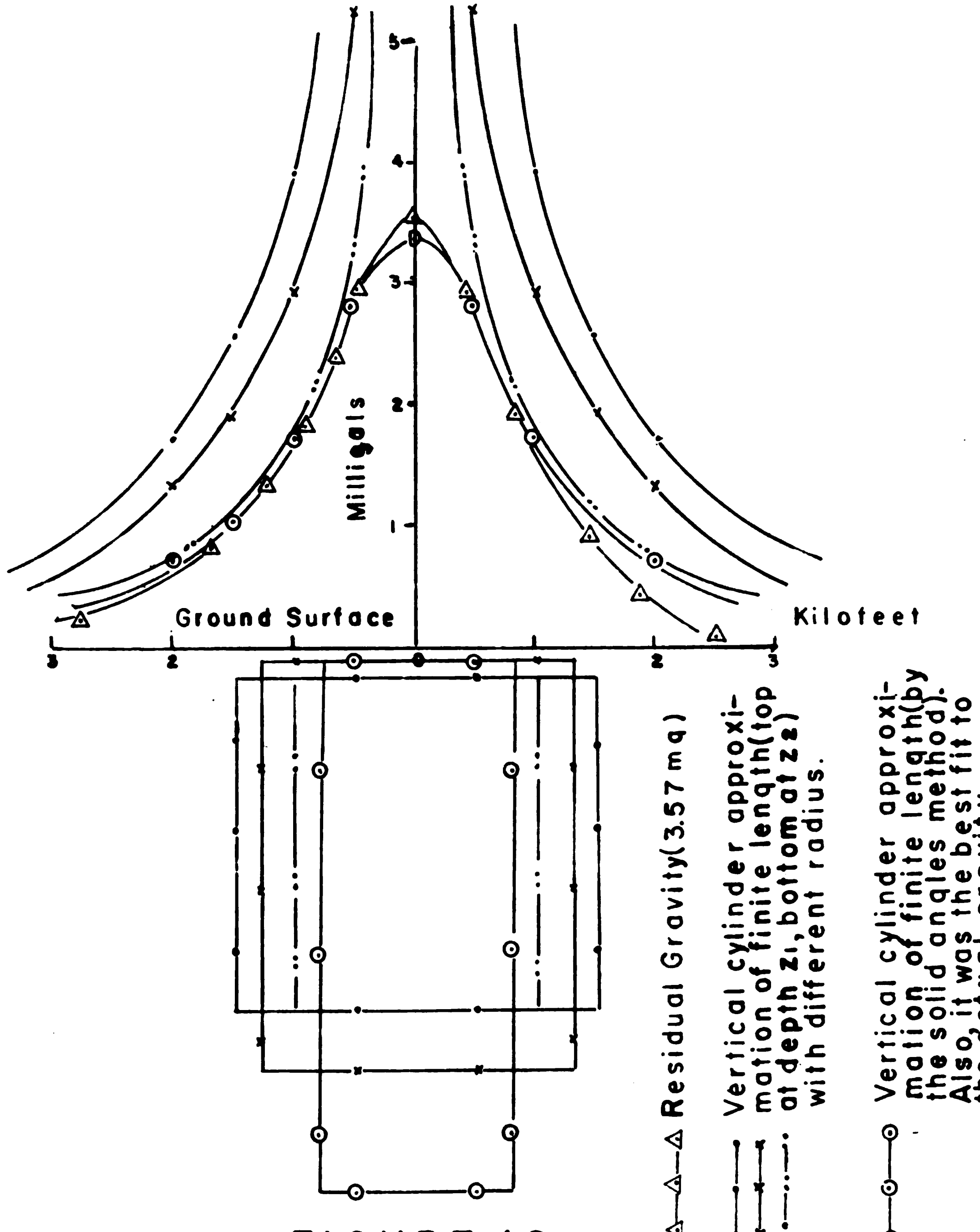

FIGURE 16

VERTICAL GRAVITY PROFILES OVER CYLINDRICAL MODELS

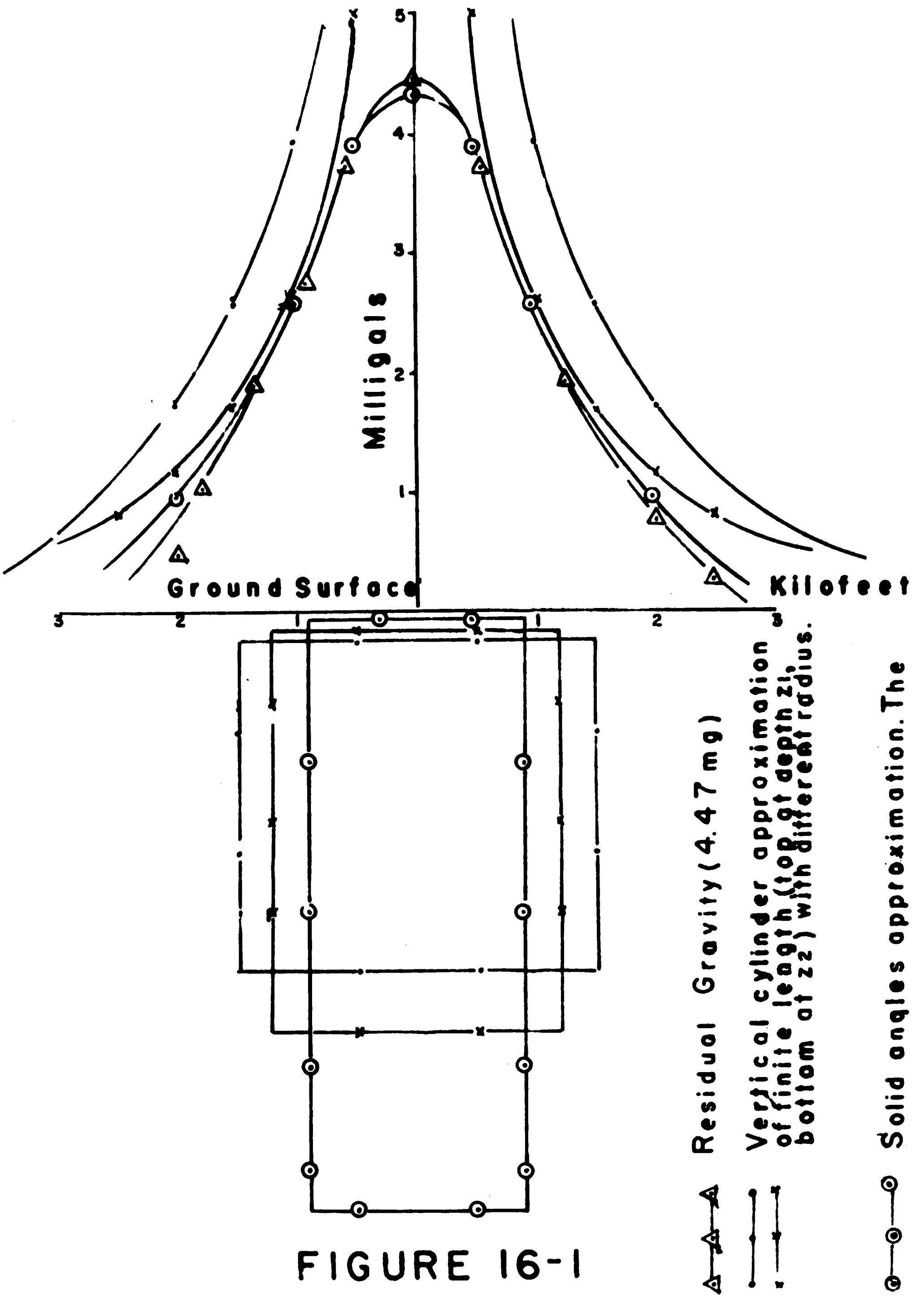

FIGURE 16-1

$$V = \pi R^2 h$$

where: V = volume in cubic Kilofeet

R = radius (.8 Kilofeet)

h = thickness or height of the cylindrical model (8.8 Kilofeet)

$$V = 3.14 \times (.8)^2 \times (8.8) = 17.7 \text{ cubic Kilofeet}$$
$$= 4.8 \times 10^{11} \text{ cm}^3$$

The excess mass was easily determined once the volume was known and the density contrast assumed. The excess mass of the cylinder was:

$$X \text{ mass} = V \times \Delta\sigma$$
$$= 4.8 \times 10^{11} \text{ cm}^3 \times .45 \text{ grams/cm}^3$$
$$= 2.2 \times 10^{14} \text{ grams}$$

These values of volume and excess mass of the cylindrical bodies may be in error because of the uncertain in the real depth to the bottom, and they only must be considered as approximations to the true values.

The cylinder that best fit the positive gravity anomaly (4.47 milligals) northeast of the area surveyed had a radius of .9 kilofeet, a depth to the top of .1 kilofeet, a depth to the bottom of 10 kilofeet (Figure 16-1). This second approximation was also possible by applying the solid angle method with a density contrast of .45 grams/cm^3 and calculating the sum of the solid angles of 11 thin circular slices to achieve also an error on the axis no greater than -6% (Figure 15). On this figure the numbers from 1-11 represent the 11 thin circular slices with different depths to the top and bottom of the theoretical cylindrical body. The radius and the density contrast had to be changed in order to best fit the theoretical gravity curve to the actual gravity. It was also apparent when calculation for finite cylindrical body was done (by the vertical line element) that the error on the axis exceeds in most cases 100% or greater, so the calculation for this method is considered very poor (Hammer, 1974). More generally, the range of maximum gravity error as a function of length and diameter of a cylinder is shown in a chart developed by Hammer (Figure 3, p. 209, 1974). The curve is plotted in dimensionless unit H/d with dimensionless unit R/d as variable parameter, where H represents the thickness or height of the cylindrical body (kilofeet), d (kilofeet) is the depth to the top, and R is the radius also in kilofeet.

Another important disadvantage in this approximation is complete lack of flexibility with respect to irregular shape and variable density. Naturally a similar method was applied to the "solid angles" approximation, using another chart developed by Hammer (1974, p. 223). The excess error on the axis was calculated for each thin slice of the theoretical cylindrical body and it was not

greater than -6%. The error on the flank can be estimated subtracting the solid angle curve approximation from the actual residual gravity. Perhaps if one more assumption (such as that the radius will be not constant throughout the intrusive body) is taken into account, a final best fitting close to the flanks of the anomalous body could be possible (Nettleton, 1942, pp. 309-310). However, the above sample will serve to show the ambiguity in the possible source of a given residual gravity curve where geological and structural controls were not well known. It will also illustrate why approximation methods such as have been outlined here are sufficiently accurate to answer most questions regarding possible sources of anomalies when other control is not available. A third gravity anomaly approximately 1 1/2 miles northeast from the center of the 4.47 milligals gravity anomaly (Figure 12-1) resulted from the gravity field measurements. This anomaly is also positive with a high and low negative to the right and left side of the 4.47 milligals gravity anomaly respectively and will not be analyzed in detail like the first two one because of its small influence over the main anomalous bodies. It will be discussed later and its possible correlation with the main bodies will be established.

CHAPTER XI

MAGNETIC INTERPRETATION

Frequent occurrence of rocks whose NRM (natural remanent magnetization) is in the direction nearly opposite to the present geomagnetic field was a puzzling fact in the early days of rock magnetism studies. Some authors have pointed out that the phenomenon could be explained by possible reversals of the earth's main magnetic field in the past. The investigation of David (1904) and Brunhes (1906) into the magnetization of lava flows and their underlying baked clay led to the first observation of directions of magnetization in rocks roughly opposed to that of the present field. This led to speculation that the earth's magnetic field had reversed itself in the past. Since then, the study of many rocks formations around the world and throughout the geological column has revealed directions of magnetization roughly opposed to one another.

The increasing amount of paleomagnetic work supports the validity of the viewpoint that the most recent world-wide reversal of the earth's magnetic field took place about 700,000 years ago during the early Pleistocene or very late Pliocene age. Hence the potential value of this reversal as a key to settling the Plio-Pleistocene boundary may well be emphasized. Intrusions of igneous rocks in nature are common, and the rocks which are intruded are reheated to some extent. This process will cause a remagnetization of the intruded rock as a result of cooling from above the Curie temperature. It had been well established that the earth's field reversed itself many times. When rocks of equal or different sources cooled or have deposited, it can produce reverse polarity at times when the earth's field has been reversed. Naturally, it will explain the present case if one body was intruded when the earth's field had different polarity.

Reversals of the Earth's Magnetic Field

Self-Reversals

Neel (1955) quoted in Strangway (1970) has considered theoretically several mechanisms by which rocks would undergo self-reversal of their remanence. He pointed out that to have self-reversals requires the coexistence and interaction of two ferromagnetic materials. These two constituents need not be different ferromagnetic materials, they may represent two interwoven sub-lattices of a ferrimagnetic.

Work by Nagata (1961) on the extract from the self-reversing Haruna dacite was pursued by Uyeda (1958) using synthetic materials. He found that self-reversal is an intrinsic property of the ilmenite-haematite solid solution series in the region of .45 to .60 ilmenite.

Other workers have showed that the reversal is connected with the ordering and disordering of Fe and Ti ions in the lattice. The magnetic characteristics of rocks having reverse NRM are the same as from those of normally magnetized rocks. Then the occurrence of such rocks having reverse NRM may most plausibly be interpreted on the hypothesis that the geomagnetic field has occasionally reversed and that the rocks were magnetized during the periods of the reverse field.

Field Reversals

Wilson (1962a) has produced a particularly convincing piece of evidence in favor of field reversal from an investigation of a doubly heated rock. A band of laterite had been heated by an overlying lava, the direction of magnetization of both agreeing and having reversed polarity. Subsequently both the laterite and the lava were intruded by a basic dike. The direction of this dike was also reversed. The second heating by the dike did not however exceed the Curie temperature, so that the heating effect could be removed by partial thermal demagnetization. As a result each laterite sample contained two independent magnetization, one for each of two different temperature ranges. In the same sample, both of these superimposed magnetization were of reversed polarity. It seems almost impossible to explain this fact by any known or theoretical self-reversed mechanism.

Strangway (1970) says that in contrast to the search for self-reversals in nature much evidence has been produced to show that the field did in fact reverse. The most convincing evidence of all has been produced by the combined study of paleomagnetism and careful isotopic age-dating, since basaltic rocks have been found to have sufficient potassium to be suitable for potassium-argon dating. In very young rocks, less than about 5 million years old, many investigators have found consistent evidence on a worldwide basis to show that reversals take place simultaneously around the world (Figure 17, data after Opdyke, 1972).

The rocks which are younger than 700,000 years show mostly "normal" polarity, if the present field is called "normal." This last period has been called the "Brunhes normal" epoch. From .7 to roughly 2.5 million years ago, the field was essentially reversed, although some interludes of normal periods have occurred. This epoch (-0.7 to -2.5×10^6 years) has been called the Matuyama reversed epoch. Before that (to -3.3×10^6 years) follow the Gauss normal epoch and (to -4.5×10^6 years) the Gilbert reversed epoch. However, in all these epochs frequent short intervals of opposite polarity ("events") to that corresponding to the character of the "epoch" occurred. The pattern of

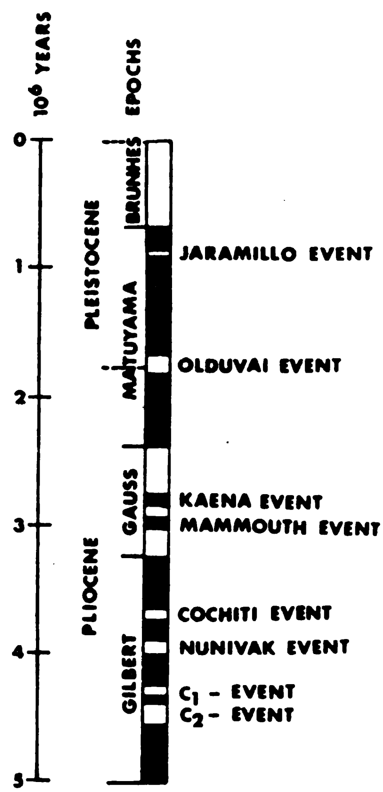

Figure 17

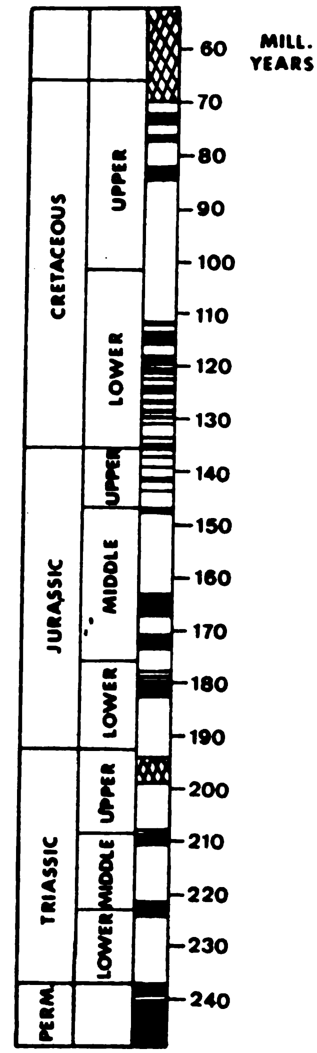

Figure 17.1

Fig. 17.--Magnetic stratigraphy during the last 5 million years. White: normal magnetization; black: reversed magnetization (data after Opdyke, 1972).

Fig. 17-1.--Field reversals from Tertiary to Permian. White: normal; black: reversed; cross-hatched: uncertain (due to frequent reversals) magnetization (data from Irving et al., 1973).

frequent back and forth reversals of the geomagnetic field with a frequency of one change in 400,000 years seems to have been the rule for about the last 70 x 10^6 years. The polarities have been followed back further to the upper Permian. The reversal frequency has apparently been much less (once in 10^7 years or more) before the Tertiary time than in the Tertiary and Quaternary (Figure 17-1, data after Irving et al).

This evidence is strong proof that the field reversals do occur, since many different rock types (basalts, sediments), and areas show consistent results. This resulted includes data from many places and several laboratories, and although additional features may yet appear, the general sequence of events for the last 5 million years (at least) is now clear.

Assumptions

On examining the magnetic anomaly contour maps of both vertical and total components, it is found that a single vertical cylinder does not suggest itself to be the best representation of the anomalous bodies. A lengthy and arduous computation such as was employed for gravity interpretation can satisfactorily explain the observed trends of the components. Figures 3-1 and 4 show the contour maps of vertical and total anomaly components respectively. A magnetic profile was drawn in the same Northeast-Southwest direction as the Bouguer gravity profile (Figure 3-1). In order to determine the magnetic susceptibility, and induced and remanent magnetization some assumptions were made. This survey will illustrate that it is very important to know the above parameters mentioned, and the ratio of remanent to induced magnetization and the direction of remanent magnetization for the correct interpretation of magnetic anomalies. In general, it is known that Jr (the remanent magnetization) is not in the direction of the present earth's field. In recent years, laboratory measurements have shown that the direction of natural remanent magnetization is parallel to the earth's present field only in rocks of Quaternary and late Tertiary ages (Girdler, 1960). This must be taken into account for the following assumption.

One of the main assumptions was done, taking into account the effect of Induced and Remanent magnetization. It is inferred that the natural remanent magnetization is much greater than the induced magnetization since one magnetic anomaly is negative. This suggests the presence of igneous rocks with a strong reverse magnetization.

In one case it was assumed that the anomaly is due to an intrusive body (which can be represented by a vertical finite cylinder), and both Jr (remanent magnetization) and Ji (induced magnetization) are parallel to the present earth's field (55,000 gammas) and therefore the cylinder will be vertically polarized. In fact the earth's magnetic field in this area has an inclination about 75-76 degrees, which means that a vertical polarization may be expected for a first approximation. In this case the formula $J = Ji + Jr$ was applied. In a second case, it was assumed that the anomaly was also due to an intrusive body (like the first one) and both Ji and Jr were parallel to the present earth's field, but not in the same sense. This assumption was made since the aeromagnetic and ground vertical maps showed the north-seeking pole pointing up (instead of down for the northern hemisphere), so the vertical component of the field gives anomalies in opposition to those to be expected from the present field. Then the formula above mentioned will be of opposite sign, $J = Ji - Jr$.

It will be seen later that the value of the angle of the lower surface will be sufficiently small not to affect any considerable change in the final calculation. If these assumptions are allowed, then the formula:

$$V = J\ (W1 - W2) \text{ gammas (Finite Cylindrical Body)}$$

where: V = residual vertical magnetic anomaly (Figures 18, 18-1)

J = intensity of magnetization (e.m.u./cm^3)

W1 = solid angle subtended by the upper surface

W2 = solid angle subtended by the lower surface

can be used to calculate the magnetic remanence, which will be of opposite sign for the two anomalies treated.

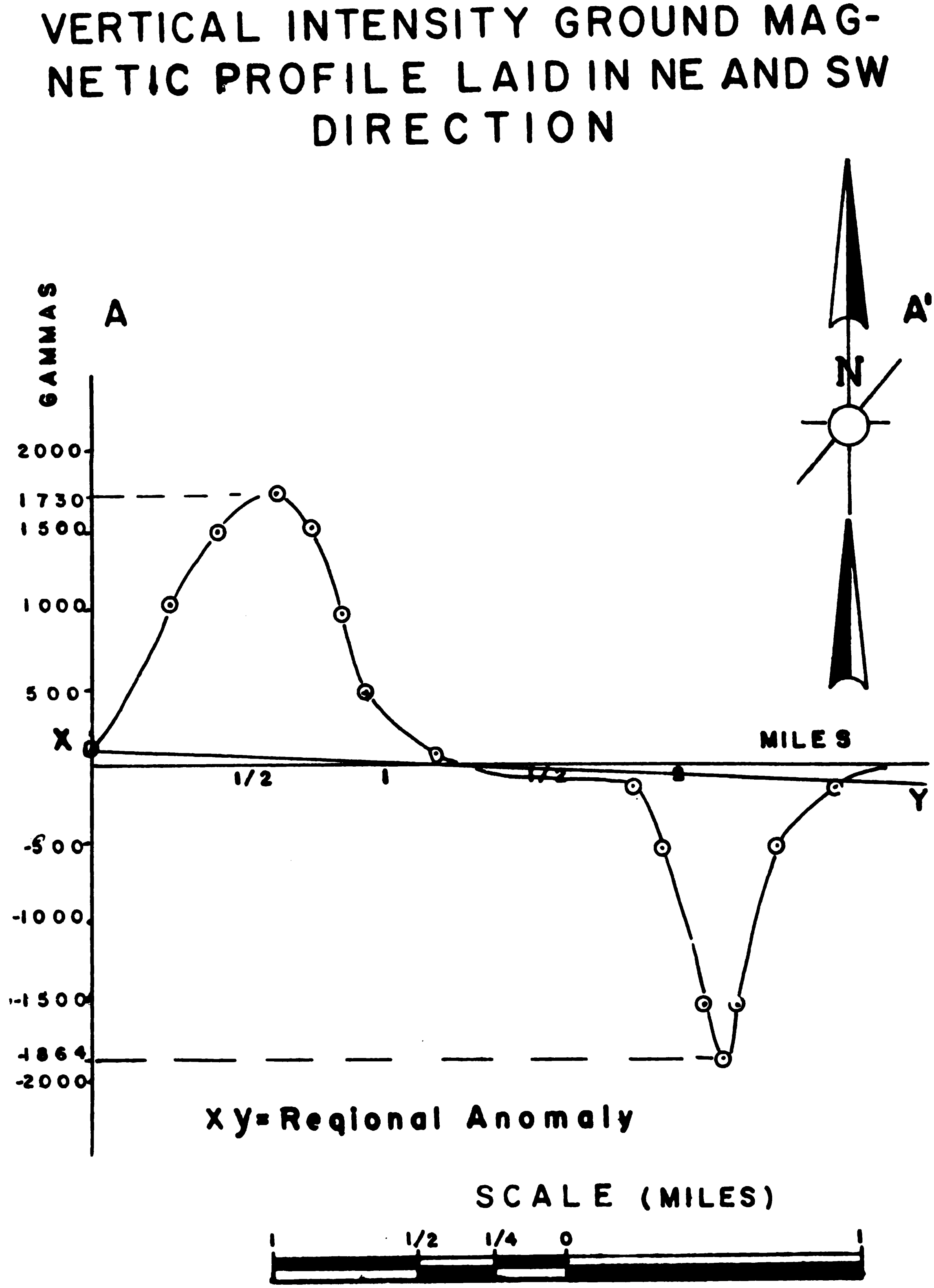

Fig. 18.--Vertical Intensity Ground Magnetic Profile Laid in Northeast and Southwest Direction.

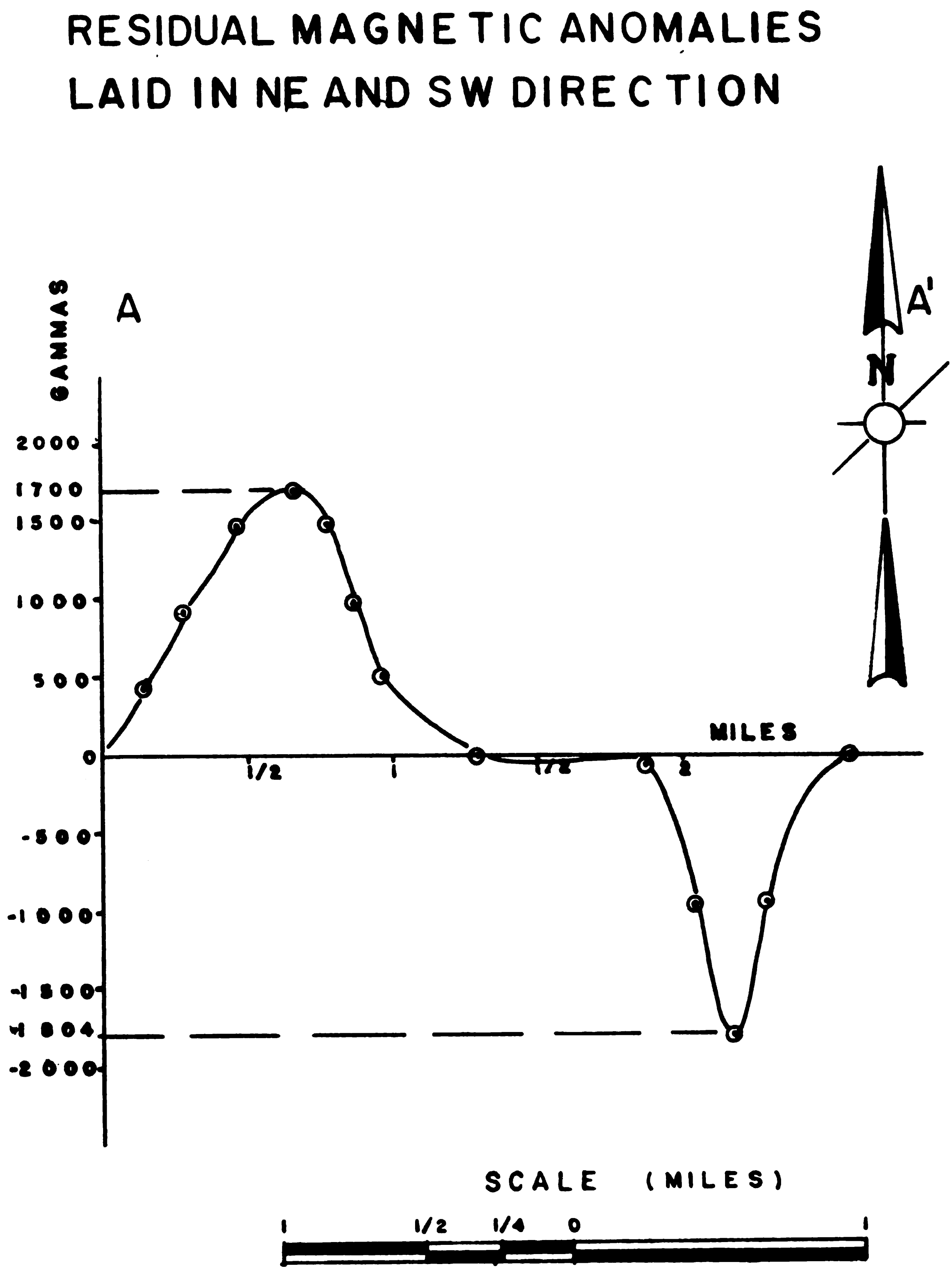

Fig. 18-1.--Residual Magnetic Anomalies Laid in Northeast and Southwest Direction.

Moreover, the application of the formula before mentioned (which is an application of the "solid angles" methodology) was so a continuation of the same technique employed in gravity interpretation. Then the margin of error will be less, and the value of the parameters so calculated will be closer to the reality. In any practical job like this (where measurements on orientated rock samples were impossible to do), several assumptions must be in mind to make the best approximation to resolve J into Jr and Ji.

Simple Method of Determining the Magnetic Susceptibility and the Induced Magnetization

The method described below is rough but very useful for obtaining quick estimates of the susceptibility and induced magnetization of magnetic rocks. For a vertically magnetized, vertical cylindrical body, the volume magnetization can be considered as replaced by a surface magnetization of its upper and lower faces. For each such face the magnetic effect at the point being considered is proportional to the solid angle subtended; hence, the magnetic effect of the cylindrical body is proportional to the difference between the solid angles subtended by its upper and lower faces. If the bodies had no components of remanent magnetization, the susceptibility contrast for the positive and negative anomalies was determined by the formula before mentioned:

$$V = J\ (W1 - W2)$$

Values for W1 and W2 were obtained from a chart (Nettleton, 1942; 1971) which was also employed for gravity interpretation. With this chart a quick estimation of the angles W1 - W2 can be done, knowing the depth to the top and to the bottom of the theoretical cylindrical bodies, so as its radius. From the gravity calculation (for the positive magnetic anomaly) these values were: Z1 equal to .1 kilofeet, Z2 equal 10 kilofeet, and R equal to .9 kilofeet. It should be understood that the value mentioned above have been applied from gravity approximation to magnetic interpretation. In other words, the size and shape of the causative gravity anomalies have been assumed to be approximately the same for the magnetic anomalies. The position and shape of the Bouguer gravity anomalies and vertical ground magnetic anomalies, surely indicated a close approximation, assuming equal dimensions for the magnetic interpretation.

From the values above mentioned, the ratio Z/R was obtained and the reading was taken on a horizontal coordinate (chart for solid angles, Nettleton, 1942; 1971) for points on axis (X = 0).

Positive Residual Relief
(1700 gammas)

The formula before mentioned was rearranged to calculate the magnetic susceptibility:

$$J = \Delta K \; HE = \frac{V}{(W1 - W2)}$$

$$\Delta K = \frac{V}{HE \; (W1 - W2)}$$

where: J = intensity of magnetization (e.m.u./cm^3)

ΔK = susceptibility contrast (e.m.u./cm^3)

V = vertical magnetic anomaly (residual, 1700 gammas)

HE = earth's magnetic field (55,000 gammas)

W1 = solid angle subtended by the upper surface (4.7) (obtained from the ratio Z1/R, equal to .25)

W2 = solid angle subtended by the lower surface (.025) (obtained from the ratio Z2/R, equal to 11.25)

The calculated value for the susceptibility contrast so calculated will be a maximum value, because the remanent magnetization was not taken into account. This value was 6.612×10^{-3} e.m.u/cm^3 units. This value of magnetic susceptibility, corresponding to the maximum measurements on 200 oriented samples from the Keweenawan gabbro, diabase, and associated rocks due by Charles (1965) near Duluth, Minnesota, may be a clue for later interpretation. The calculated value for Ji, the induced magnetization, in a magnetic field of 55,000 gammas is 3.64×10^{-3} e.m.u/cm^3 units.

Negative Residual Relief
(-1804 gammas)

A similar calculation was done with W1 equal to 5.5, W2 equal to .028. The calculated value for ΔK (the magnetic susceptibility contrast) was 5.994×10^{-3} e.m.u/cm^3 units. The calculated value for Ji, the induced magnetization, in a magnetic field of 55,000 gammas was 3.29×10^{-3} e.m.u/cm^3 units.

Method to Determine the Remanent Magnetization of Approximately Cylindrical Bodies

Once an approximated maximum susceptibility contrast was determined by the method outlined before, the effect of induced and remanent magnetization was applied. The formula J = Ji ± Jr will depend upon whether the induced intensity, Ji, has the same or the opposite direction as the remanent intensity, Jr. Suppose that to start with J = Ji + Jr for the vertical residual positive anomaly (1700 gammas), and then for the residual negative anomaly, J = Ji - Jr. To continue with the application of induced and remanent magnetization, and looking the values of susceptibility contrast and induced magnetization calculated before, it was concluded that:

(1) The calculated values for the susceptibility contrast were almost the same.

(2) Therefore, the induced magnetization were also almost the same.

(3) The above mentioned conclusions were expected, since the high and low total and vertical magnetic intensity maps (Figures 3-1 and 4) showed almost the same range of magnitude. It tells us that

the induced magnetization for both anomalous bodies will be the same.

So, for the second calculation, to interpret these anomalies the best possible, several susceptibility values were assumed. Naturally, these values of susceptibility contrast were chosen according to magnetic susceptibility measurements, which have been already made around the area surveyed (Meshref and Hinze, 1970; Charles, 1965).

First of all, this range of susceptibility contrasts was assumed taking into consideration that the anomalous bodies are Keweenawan basic intrusives rocks. Meshref (1970) gave an average of susceptibility (K), for intrusives (basic) of 5.683 x 10^{-3} e.m.u/cm^3, while Charles (1965) gave an average range from 0.3 x 10^{-3} to 6.0 x 10^{-3} e.m.u/cm^3. It is apparent that there exists a strong correlation between these two values which were calculated from different sites, but for equal rock formations. Susceptibility contrast values (ΔK), were assumed taken in consideration those maximum values of susceptibility (K) given by Meshref (1970) and Charles (1965).

The Koenigsberger ratio was also taken into account, and each calculation for different susceptibilities, were compared with those observed by the above mentioned workers.

So, to interpret these anomalies the best possible, a susceptibility contrast of 1.9 x 10^{-3} e.m.u/cm^3 was assumed to be the best representative average value for these two anomalies. This arbitrary value was used by the writer after several calculations, with different susceptibility contrasts, were made. Naturally, it was a lengthy and arduous computation employed to find the best representative susceptibility contrast value. Values, below 1×10^{-3} e.m.u/cm^3 were discarded because of the high Q (Koenigsberger ratio) values that they produce and which do not agree with those already calculated by Hinze et al. (1966). Also, we must have in mind that (Q) of igneous rocks is usually between 2-10, and it will exceed 100 in some basaltic effusives; also, it rarely is below unity (Nagata, 1961). In our case, any value between 2-10 will be acceptable according to the data given by Hinze (1966). He made several calculations in an external field of .6 Oersted for Keweenawan and pre-Keweenawan rocks, finding a maximum value of 10 for pre-Keweenawan iron formation. Also the gravity interpretation and the available geological information of the surrounding area were useful to choose approximately the intrude rock type. With the new susceptibility contrast (1.9×10^{-3} e.m.u/cm^3), a final approach was done. The induced magnetization so calculated gave a value of 1.05×10^{-3} e.m.u/cm^3. With this new approach, the formula: $V = J\ (W1 - W2)$, was again applied taking into consideration that J will be different for both anomalous bodies. Rearranged the formula above mentioned to calculate the remanent magnetization for the positive magnetic anomaly:

$$V = (Ji + Jr) \times (W1 - W2)$$

where V is the vertical component of the magnetic anomaly (1700 gammas), Ji is the induced magnetization (1.05×10^{-3} e.m.u/cm^3), Jr is the remanent magnetization, and W1 - W2 are the angles subtended by the upper and lower surfaces (4.68). The remanent magnetization gave a value of 2.58×10^{-3} e.m.u/cm^3. A similar calculation was done for the negative magnetic anomaly where V has a value of -1804 gammas, Ji is 1.05×10^{-3} e.m.u/cm^3, and W1 - W2 is 5.47. The remanent magnetization gave a value of -4.24×10^{-3} e.m.u/cm^3.

Koenigsberger Ratio Calculation (Q = Jr/Ji)

Vacquier (1961) suggested that, by carefully repeating a survey across the span of a decade in regions where the secular variation is pronounced, it might be possible to determine in situ the ratio of remanent to the induced polarization, given rise to large magnetic anomalies. After the induced and remanent magnetization were calculated, a quick approximation of their ratio was done to indicate the range within which its value falls. This approximation was possible applying the formula: Q = Jr/Ji, where Ji is the magnetization induced in the sample by the earth's magnetic field (HE) at the surveyed area, and Jr the remanent magnetization. Quantities Jr, Ji and K were expressed on a volume basis in c.g.s units throughout this work. From the formula before mentioned (Q = Jr/Ji), it was found, for the positive residual magnetic anomaly (Figure 17-1) a value of 2.46, and for the negative residual magnetic anomaly, a value of 4.04. A summary of magnetic properties (after Hinze, O'Hara, Secor and Trow, Report of Investigation No. 12, Michigan Geological Survey, 1966) was done, and the Koenigsberger ratio was calculated for rocks of Keweenawan and pre-Keweenawan ages in an external field of .6 Oersted (60,000 gammas). If a comparison is established between them and the present calculation, it will be seen that the rock type of the area surveyed may be considered of Keweenawan age (basic intrusives), naturally taking into consideration that the susceptibility contrasts were assumed from the range established for this kind of rock type, given by Hinze and O'Hara (1966). Also, the Koenigsberger ratio for both anomalous bodies were compared with those given by the above mentioned workers. Those values so calculated resulted in greater than the maximum calculated for basic intrusives (2.0). This difference may be due to the external field of .55 Oersted (55,000 gammas) which will be different than that applied by Hinze et al. (1966).

Magnetite Content (Fe_3O_4)

Magnetite is by far the most common and most magnetic of the magnetic minerals. It is probable that the magnetic properties of most rocks are directly dependent on the amount of magnetite that they contain.

Slichter's (quoted in Dobrin, 1960) careful study of the properties of magnetite indicates that its effective susceptibility in a field of the strength of that of the earth's when in powdered and highly disseminated form, as it would be expected to occur as a constituent of rock is around .3 (i.e., $300{,}000 \times 10^{-6}$) c.g.s. units. Probably it is the most useful figure for our consideration until it is only a small fraction of the total rock volume. On this basis it might be possible to estimate the percentage (by volume) of disseminated magnetite (Nettleton, 1940; 1942).

From the general formula: $J = Ji \pm Jr$, the amount of magnetite was calculated. Rearranging this formula, an approximation was done as follows:

$$J = K\ HE + Q\ K\ HE = K\ (1 + Q)\ HE$$

$$= .3\ P\ (1 + Q)\ HE \text{ (for the positive magnetic body)}$$

$$= .3\ P\ (1 - Q)\ HE \text{ (for the negative magnetic body)}$$

For the positive magnetic body:

$$.017 = .3\ P\ (1 + 2.46)\ .55$$

$$P = .029 = 2.9\% \text{ (magnetite by volume)}$$

For the negative magnetic body:

$$-.01804 = .3\ P\ (1 - 4.04)\ .55$$

$$P = .035 = 3.5\%\ \text{(magnetite by volume)}$$

Parasnis (1975) calculated percentages of rocks and ores with a maximum value of 3.4% of magnetite for basic rocks. Taking into account these values and comparing with the above calculated, it will be seen that the present percent of magnetite in the actual rock will be in this range observed by Parasnis. However it must be remembered that in any particular case these values may differ enormously, depending on the amount of magnetite and grain size.

CHAPTER XIII

CONCLUSION

Approximations Made

One of the most important approximations made in the gravity model interpretation was that the observed gravity highs were approximated by cylindrical vertical bodies using two different methods (the vertical line method and the solid angles method). The approximation was made assuming structures of approximately circular cross section, varying the density, size, and shape of the stocked cylindrical bodies. The volume and excess mass calculated from the best model (Figure 16 and 16-1) was slightly higher for one body than the other. In both cases, these values should not be considered exact, because of the causative error due to the application of the solid angles methods, and the possible error due to the calculation of the other parameters, like depth, size, density contrast, etc.

Secondly, approximations were made with different density contrasts using a maximum value of .45 grams/cm^3. This is a high value of density contrast, corresponding to a body considerably denser than the surrounding rock.

Values like this have been found by Bacon (Michigan Geological Survey, personal report) at the eastern half of the Northern Peninsula of Michigan. However this high value which is suggestive of a more basic and more dense rock type is meant to represent a basic rock such as gabbro or diabase, intruding rock of lower density. It is important to remember that a body need not have a uniform density contrast throughout it as was assumed for the best final fitting models.

One more approximation made for the present work was the calculation of remanent magnetization, assuming a susceptibility contrast of 1.9×10^{-3} e.m.u/cm^3. Using this value and having in mind that the direction due to the earth's vertical magnetic field will be unchanged but that of the remanence will be reversed (for the negative magnetic anomaly), an approximation of Jr was carried out for both anomalous bodies. This calculation of remanent magnetization showed that it was stronger than the induced magnetization in both anomalous bodies. Also, the remanent magnetization of the (-) body is stronger than the first one (positive anomaly). This value was expected by the writer because of the reverse magnetization that occurs there. This value may not be sufficiently high to represent the best possible the negative magnetic anomaly. However, we must understand that in any practical job, where several assumptions have been made (because of the unknown geology and the real susceptibility contrasts), a margin of error must be expected.

The Reverse Nature of Anomaly Related to Geology

(1) the negative magnetic anomaly shown by the aeromagnetic map (U.S. Geological Survey, 1970, Figure 4) and by the vertical intensity ground magnetic map (Figure 3-1) might be explained by greater remanent magnetization having opposite direction to that of the induced magnetization.

(2) The negative anomaly is everywhere magnetized in a direction opposite to the present field whereas older and younger bodies nearby showed apparently directions of magnetization conforming to the present day field. As the south-seeking pole points down (-1804 gammas) instead of up for the northern hemisphere, the vertical component of the field gives anomalies in opposition to those to be expected from the present field.

(3) The depth and shape of the best fit cylindrical gravity models, their density contrasts, and their high magnetite content, suggested to the writer that the anomalous bodies may be intrusive basaltic rocks within the granitic basement.

(4) Quantitative interpretation is further handicapped because the proportion of induced and remanent magnetization is rarely well known (Heiland, 1940). The

above statement still holds true in general for an area with complex Precambrian geology such as the Upper Peninsula of Michigan.

(5) This study has shown in conclusion that aeromagnetic interpretation together with gravity and magnetic ground survey, are extremely useful tools in estimating approximately the local structure of Precambrian terrain consisting of widely diverse magnetic formations. However the complexity of the magnetic rock properties (like susceptibility contrast, induced and remanent magnetization) reduce the interpretation to a semiquantitative approach based upon the integration of several factors. These factors, like surface and subsurface geology interpretation, Bouguer gravity anomalies and analytical studies of gravity and magnetic data will be useful for the final interpretation. Analytical studies useful in the interpretation include gravity and magnetic depth determinations and trend analysis, total and theoretical intensity anomalies, and correlation of theoretical magnetic and gravity anomalies with the observed gravity and magnetic data.

In reality, how deep those intrusive bodies can prevail will be a geological problem. It might suffice to pay more attention to the possible density contrast of the intruded bodies and the surrounding rocks and also to the susceptibility contrast of them.

It will be interesting to continue with this research, since the purpose of gravity and magnetics is simply to localize interesting anomalous areas and give approximate values of properties to the causative anomalous bodies. Further exploration with seismograph and borehole drilling would be interesting to obtain a better evaluation of the shape and size of these anomalous bodies.

APPENDIX I

DATA TABLE--GRAVITY

APPENDIX I

DATA TABLE--GRAVITY

Stn	Elev feet	Free-Air, Bouguer, Drift and Latitude corr (Gravity) mgals	Bouguer Gravity mgals	Approximate Location
W-1	816	4401.53	0	W1-W17, westward
W-2	848	4401.95	+0.42	along the main
W-3	817	4399.94	-1.59	medium duty road
W-4	817	4400.00	-1.53	(base line, which
W-5	822	4399.80	-1.73	cut the grid pat-
W-6	832	4400.02	-1.51	tern in exactly
W-7	840	4400.76	-0.77	half).
W-8	872	4401.88	+0.35	Interval, 1/4 mile
W-9	863	4401.55	+0.02	
W-10	843	4400.64	-0.89	
W-11	828	4400.34	-1.19	
W-12	829	4399.85	-1.68	
W-13	853	4400.15	-1.38	
W-14	888	4401.46	-0.07	
W-15	868	4401.25	-0.28	

Stn	Elev feet	Free-Air, Bouguer, Drift and Latitude corr (Gravity mgals	Bouguer Gravity mgals	Approximate Location
W-16	870	4401.58	+0.05	
W-17	852	4403.17	+1.64	
N-18	849	4400.17	-1.36	N18-N22, northward
N-19	879	4399.52	-2.01	perpendicular to the
N-20	875	4399.02	-2.51	base line, right from
N-20	875	4399.34		station number seven,
N-21	885	4401.53	+2.19	interval, 1/4 mile.
N-22	882	4400.82	+1.16	
N-23	880	4402.21	+2.55	N-23-N24, northward
N-24	861	4400.57	+0.91	perpendicular to the
				base line, right from
				stations six and five
				respectively, 1 1/2
				mile from base line
N-25	872	4400.87	+1.21	N25, northward
N-26	844	4398.48	-1.18	perpendicular from
N-27	892	4403.43	+3.77	base line, right from
				station four, 1.75
				miles from it.
				N26, exactly two miles
				from station one,

Stn	Elev feet	Free-Air, Bouguer, Drift and Latitude corr (Gravity) mgals	Bouguer Gravity mgals	Approximate Location
				northward
				N27, northward perpendicular to the station number nine, this station has the maximum + gravity value, 1/4 mile from station nine.
N-19	879	4399.86		Base station
N-28	864	4399.14	-1.06	N28, half mile from
N-29	820	4397.60	-2.60	station eight
N-30	853	4402.30	+2.10	N29, 1/4 mile from station eight
				N30, half mile from station nine
N-31	820	4395.87	-4.33	N31, 1/4 mile from station six
N-32	819	4398.33	-1.87	N32-N34, perpendicular
N-33	817	4398.42	-1.78	to the station number
N-34	819	4398.07	-2.13	five every 1/4 mile.
N-35	826	4397.47	-2.73	N35, .75 mile from station six

Stn	Elev feet	Free-Air, Bouguer, Drift and Latitude corr (Gravity) mgals	Bouguer Gravity mgals	Approximate Location
N-36	818	4397.15	-3.05	N36, half mile from six
N-37	841	4397.24	-2.96	N37, one mile from six
N-38	826	4397.66	-2.54	N38, 1 1/4 mile from six
N-39	892	4398.81	-1.39	N39, 1 1/4 mile from five
N-40	853	4399.43	-0.77	N40, 1 mile from five
N-41	824	4398.09	-2.11	N41, .75 mile from eight
N-42	830	4399.94	-0.26	N42-N43, perpendicular to 9, .75 and 1 mile
N-43	836	4399.49	-0.71	from it.
N-44	834	4398.26	-1.94	N44, 1 mile from eight (northward, perpendicularly)
N-45	827	4400.32	+0.12	N45-N48, perpendicular
N-46	832	4401.07	+0.87	to 10 (northward)
N-47	832	4399.68	-0.52	
N-48	844	4400.80	+0.60	
N-49	842	4398.31	-1.89	N49-N52, northward

Stn	Elev feet	Free-Air, Bouguer, Drift and Latitude corr (Gravity) mgals	Bouguer Gravity mgals	Approximation Location
N-50	855	4399.23	-0.48	perpendicular to 13,
N-51	830	4399.67	-0.18	interval, 1/4 mile
N-52	878	4399.23	-0.97	
S-53	826	4400.99	+0.79	S53, southward from 11, interval, 1 mile
S-53	826	4401.51		Base station
E-54	826	4400.91	-1.12	E54-E58, eastward
E-55	812	4400.30	-1.73	from 53, interval
E-56	811	4399.96	-2.07	1/4 mile
E-57	815	4399.29	-2.74	
E-58	816	4399.63	-2.40	
S-59	817	4399.68	-2.35	S59, southward from E58, interval, 1/4 mile
S-60	814	4400.62	-1.41	S60, southward from 11, interval, .75 mile
W-61	813	4400.75	-1.28	W61-W66, westward
W-62	814	4401.48	-0.55	from S60, interval,
W-63	822	4402.56	+0.53	1/4 mile
W-64	827	4402.71	+0.60	
W-65	825	4401.85	-0.18	
W-66	818	4402.00	-0.03	

Stn	Elev feet	Free-Air, Bouguer, Drift and Latitude corr (Gravity) mgals	Bouguer Gravity mgals	Approximation Location
S-67	817	4402.29	+0.26	S67-S69, southward
S-68	818	4403.04	+1.01	from W65, interval,
S-69	836	4401.32	-0.71	1/4 mile
W-70	833	4401.69	-0.34	W70, westward from S69, interval, 1/4 mile
E-71	827	4401.27	-0.76	E71, eastward from S69, interval, 1/4 mile
S-72	833	4400.63	-1.40	S72-S73, southward
S-73	814	4401.43	-0.60	from S53, interval 1/4 mile
W-74	826	4399.78	-2.25	W74-W75, westward
W-75	839	4400.66	-1.37	from S73, interval, 1/4 mile
S-76	848	4400.92	-1.11	S76, southward from S74, interval, 1/4 mile
S-77	815	4400.43	-1.60	S77, southward from S75, approximately .37 mile
W-78	832	4401.32	-0.71	W78, westward from S75, interval, 1/4

Stn	Elev feet	Free-Air, Bouguer, Drift and Latitude corr (Gravity) mgals	Bouguer Gravity mgals	Approximate Location
				mile
E-79	821	4401.88	-0.15	E79, eastward from
				S68, interval, 1/4
				mile
S-80	825	4399.88	-2.15	S80-S81, southward
S-81	828	4400.21	-1.82	11, interval, 1/4
				mile
W-82	829	4399.65	-2.38	W82, westward from
				N51, interval, 1/4
				mile
W-83	818	4399.57	-2.46	W83, westward from
				N52, interval, .75 mile
N-84	810	4399.33	-2.70	N84-N87, northward
N-85	808	4399.17	-2.86	from W83, interval
N-86	831	4399.20	-2.83	1/4 mile
N-87	826	4399.71	-2.32	
88	-	--	-	Missing point
W-11	828	4400.87		Base station
N-89	836	4401.66	+0.25	N89-N90, northward
N-90	846	4402.04	+0.64	from W11, interval,
				1/4 mile
N-91	822	4399.90	-1.50	N91, .75 mile from W12

Stn	Elev feet	Free-Air, Bouguer, Drift and Latitude corr (Gravity) mgals	Bouguer Gravity mgals	Approximate Location
N-92	836	4401.13	-0.27	N92, 1/4 mile from W12
W-12	829	4400.60		Base station
N-93	837	4399.97	-1.38	N93, 1/2 mile from W12
W-94	870	4401.41	+0.06	W94, westward from N91, interval, .12 mile
N-95	864	4402.45	+1.10	N95, 1 mile from W12
N-96	860	4400.29	-1.06	N96, northward from W14, interval, 1/4 mile
N-97	843	4401.81	+0.46	N97, northward from W14, interval, 1/2 mile
W-98	852	4403.21	+1.86	W98, westward from N97, interval, 1/4 mile
S-99	881	4400.75	-0.60	S99, southward from W98, interval, 1/4 mile
W-7	840	4401.59		Base station
S-100	859	4402.63	+0.21	S100-S101, southward
S-101	856	4402.58	+0.16	from W7, 1/4 and .37

Stn	Elev feet	Free-Air, Bouguer, Drift and Latitude corr (Gravity) mgals	Bouguer Gravity mgals	Approximate Location
				mile interval respectively
S-102	828	4400.31	-2.11	S102-S104, southward
S-103	849	4402.25	-0.17	from W8, interval,
S-104	848	4402.79	+0.37	1/4 mile
W-105	852	4402.27	-0.15	W105, westward from S103, interval, 1/4 mile
S-106	824	4400.14	-2.28	S106-S107, southward
S-107	812	4399.34	-3.08	from W6, 1/4 and .37 mile respectively
S-108	825	4400.05	-2.37	S108-S109, southward
S-109	842	4402.03	-0.39	from W7, 1/2 and .75 mile respectively
S-110	832	4400.77	-0.65	S110, southward from W9, 1/4 mile interval
S-111	843	4401.99	-12.3	S111, southward from S53, 2 mile interval
W-112	857	4401.25	-1.17	W112, westward from S110, 1/4 mile interval
W-11	828	4400.96		Base station
W-113	810	4401.45	-0.13	W113-114, westward

Stn	Elev feet	Free-Air, Bouguer, Drift and Latitude corr (Gravity) mgals	Bouguer Gravity mgals	Approximate Location
W-114	808	4402.08	+0.50	from S110, 1 1/2,
W-115	831	4402.17	+0.59	1.75 and 2 miles respectively
S-116	826	4401.87	+0.29	S116, southward from W115, 1/4 mile
E-117	855	4402.25	+0.67	E117-119, eastward
E-118	836	4401.99	+0.41	from W113, 1/4 mile
E-119	846	4400.75	-0.83	interval
S-120	822	4401.54	-0.04	S120, southward from W12, 1/2 mile interval
S-121	836	4402,08	+0.50	S121, southward from W13, 1/2 mile interval
W-1	816	4403.11	0	Base station
S-122	812	4399.93	-3.18	S122, southward from E54, 1 1/4 mile inter-val right to the bottom outside of the grid pattern
E-123	825	4399.65	-3.46	E123, eastward from S122, approximately .12 mile outside of the grid pattern

Stn	Elev feet	Free-Air, Bouguer, Drift and Latitude corr (Gravity) mgals	Bouguer Gravity mgals	Approximate Location
E-124	842	4399.97	-3.14	E124-125, eastward
E-125	832	4399.46	-3.65	from E123, right to the bottom along the 2 mile line from the medium duty road
N-126	843	4400.09	-3.02	N126-128, northward
N-127	857	4400.51	-2.60	from E125, 1/4 mile
N-128	837	4400.97	-2.14	interval
W-129	845	4401.10	-2.01	W129, westward from N128, 1/4 mile interval
N-130	831	4401.70	-1.41	N130, .12 mile interval
S-131	849	4401.01	-2.10	S131, 1/4 mile from W129
S-132	892	4401.75	-1.36	S132, .75 mile from E55.
S-133	869	4399.66	-3.45	S133, southward from E54, approximately .60 mile interval
W-1	816	4403.12		Base station
N-134	825	4403.67	+0.54	N134-137, northward
N-135	810	4402.23	-0.90	from W17, 1/4 mile

Stn S	Elev feet	Free-Air, Bouguer, Drift and Latitude corr (Gravity) mgals	Bouguer Gravity mgals	Approximate Location
N-136	802	4401.20	-1.93	interval
N-137	822	4401.34	-1.79	
N-138	893	4402.09	-1.03	N138-139, northward
N-139	822	4401.81	-1.32	from W16, .75 and 1/2 mile interval respectively
N-140	842	4400.57	-2.55	N140, 1/4 mile from N95
N-141	818	4401.18	-1.94	N141, approximately 1 mile from N90
N-142	844	4400.24	-2.88	N142, 1/4 mile from N141
N-143	837	4400.35	-2.57	N143, .75 mile from N52
N-144	807	4399.87	-3.25	N144, .85 mile from W82
N-145	810	4400.11	-3.01	N145, .55 mile from W82
S-146	822	4403.81	+0.69	S146-149, southward
S-147	842	4403.57	+0.45	from W1, 1/2 mile
S-148	824	4403.88	+0.76	interval (146-147
S-149	846	4403.80	+0.68	outside of the grid

Stn	Elev feet	Free-Air, Bouguer, Drift and Latitude corr (Gravity) mgals	Bouguer Gravity mgals	Approximate Location
				pattern
E-150	846	4403.66	+0.54	E150, 1 1/4 mile from N126
N-151	832	4403.59	+0.47	N151, 1/4 mile from E150
W-152	816	4406.32	+3.20	W152, 1/2 mile from S53

APPENDIX II

DATA TABLE--MAGNETIC

APPENDIX II

DATA TABLE--MAGNETIC

Stn	Meter Corrected Readings (Gammas)	Approximate Location
W-1	0	W1-W17, westward along the main duty road (base line for Gravity Readings)
W-2	-22	
W-3	-53	
W-4	-14	
W-5	+4	
W-6	+33	
W-7	-149	
W-8	-1601	
W-9	-204	
W-10	+214	
W-11	+233	
W-12	+182	
W-13	+31	
W-14	+30	
W-15	+18	
W-16	-34	

Stn	Meter Corrected Readings (Gammas)	Approximate Location
W-17	+153	
N-18	+263	N18-N24, the same location as
N-19	+72	Gravity stations N18-N24
N-20	-102	
N-21	+3	
N-22	+107	
N-23	+134	
N-24	+116	
N-25	+167	N25-N28, the same location as
N-26	+150	Gravity stations (N49-N52)
N-27	+130	perpendicular to W13
N-28	+182	
N-29	+183	N29-N33, the same location as
N-30	+45	Gravity stations (w83, N84-N87)
N-31	+147	
N-32	+98	
N-33	+190	
S-34	+360	S34, the same location as
E-35	+641	Gravity station (S53)
E-36	+392	E35-E37, the same location as
E-37	+343	Gravity stations (E54-E56)
N-38	-16	N38 = N35 (Gravity station)
N-39	-1604	N39-N40 = N27-N30 (Gravity

Stn	Meter Corrected Readings (Gammas)	Approximate Location
N-40	-1383	station)
S-41	+1730	S41-W45 = W62-W66 (Gravity
W-42	+998	station)
W-43	+299	
W-44	-1	
W-45	+51	
S-46	+42	S46-S47 = S67-S68 (Gravity
S-47	+453	station)
E-48	+53	E48 = W70 (Gravity station)
E-49	+250	E49 = S69 (Gravity station)
E-50	-43	E50 = E71 (Gravity station)
E-51	+148	E51 = W78 (Gravity station)
E-52	+88	E52 = W75 (Gravity station)
E-53	+9	E53 = W74 (Gravity station)
E-54	+109	E54 = S73 (Gravity station)
N-55	+90	N55 = S72 (Gravity station)
N-56	+12	N56 = S60 (Gravity station)
W-57	+263	W57 = W61 (Gravity station)
N-58	+13	N58 = S80 (Gravity station)
N-59	-635	N59 = S81 (Gravity station)
N-60	+341	N60-N66 = N89-N93, W94, N95
N-61	+351	(Gravity station respectively
N-62	+216	

Stn	Meter Corrected Readings (Gammas)	Approximate Location
N-63	+248	
N-64	+212	
N-65	+204	
N-66	+140	
N-67	+246	N67-S70 = N96, N97, W98, S99
N-68	+140	(Gravity station respectively)
W-69	+162	
S-70	+117	
S-71	+61	S71-S80 = S100-S109 (Gravity
S-72	+41	station respectively)
W-73	+201	
S-74	+51	
S-75	+51	
S-76	+151	
S-77	+11	
S-78	+21	
S-79	+51	
S-80	+81	
W-81	+151	W81-W86 = S110-W115 (Gravity
S-82	+151	station)
W-83	+151	
W-84	-57	
W-85	+83	

Stn	Meter Corrected Readings (Gammas)	Approximate Location
W-86	+83	
S-87	-343	S87-W92 = S116-S121 (Gravity
E-88	-442	station)
E-89	-512	
E-90	-217	
S-91	+13	
W-92	+256	
N-93	-1564	N93-N96 = N45-N48 (Gravity
N-94	+446	station)
N-95	+276	
N-96	+166	
N-97	+156	N97 = 1/4 mile from Gravity
		station N43
S-98	+96	S98-S99 = N43-N44 (Gravity
E-99	-54	station)
S-100	-44	S100 = N42 (Gravity station)
E-101	-384	E101 = N41 (Gravity station)
S-102	-284	S102 = N28 (Gravity station)
S-103	-454	S103 = N29 (Gravity station)
S-104	-514	S104-S106, station points between
S-105	-1254	S103-N39 (Magnetic stations),
S-106	-1854	southward, close to one of the
		magnetic anomalous bodies.

Stn	Meter Corrected Readings (Gammas)	Approximate Location
S-107	-50	S107-S118 = S122-S133 (Gravity
E-108	-50	stations). Stations 107 and 108
E-109	+30	outside of the grid pattern
E-110	±0	(see Figure 3)
N-111	+125	
N-112	+73	
N-113	-62	
W-114	+22	
N-115	+44	
S-116	+84	
S-117	+88	
S-118	+92	
N-119	+405	N119-N124 = N134-N139 (Gravity
N-120	-26	station)
N-121	-5	
N-122	+15	
N-123	+30	
N-124	-10	
N-125	-134	N125-N130 = N140-N145 (Gravity
N-126	-70	station), left corner of the
N-127	-150	grid pattern, northward
N-128	-183	
N-129	-152	

Stn	Meter Corrected Readings (Gammas)	Approximate Location
N-130	+45	
S-131	+452	S131-W137 = S146-W152 (Gravity
S-132	-85	stations), S131-132, outside of
S-133	-210	the grid pattern.
S-134	-26	
E-135	-142	
N-136	-34	
W-137	+1730	W-137 (Positive higher magnetic value)

BIBLIOGRAPHY

BIBLIOGRAPHY

Acharya, N. "Interpretation of Local Magnetic Anomalies of an Iron Ore Deposit in Podagada Range of Hills near Umerkote, Koraput District Orissa." Bulletin of the National Geophysical Research Institute of Hyderabad (NGRI), Vol. 7, pp. 1-73, 1969.

Ade-Hall, J. M. & Wilson, R. L. Petrology and Natural Remanence of the Mull Lavas. Nature, 198, pp. 659-60, 1963.

Ade-Hall, J. M. & Wilson, R. L. Opaque Petrology and Natural Remanence Polarity in Mull (Scotland) Dykes. Geophysics. J. Roy. Astron. Soc., pp. 333-52, 1969.

Anderson, T. D. "Round Lake Gravity Anomaly, Delta County, Michigan." M.S. Thesis, Michigan State University, 1974.

Bacon, L. O. Relationship of Gravity to Geologic Structure in Michigan's Northern Peninsula. Personal report in cooperation with Michigan Geological Survey, 1956.

Balsley, J. R. & Buddington, A. F. Iron-Titanium Oxide Minerals, Rocks and Aeromagnetic Anomalies of the Adirondack Area, New York. Econ. Geol., pp. 777-805, 1958.

Bayley, R. W. et al. "Geology of the Menominee Iron-Bearing District, Dickinson County, Michigan and Florence and Marinette Counties, Wisconsin." U.S. Geological Survey, Prof. Paper 513, 1966.

Blackett, P. M. S. "Lectures on Rock Magnetism." Jerusalem: Weizmann Science Press of Israel, 1956.

Breed, C. B. et al. "The Principles and Practice of Surveying." Vol. II, 8th ed. New York: John Wiley & Sons, 1962.

Brunhes, B. "Recherches Sur la direction d'aimantation des roches volcaniques. Physics, vol. 5, pp. 705-24, 1906.

Bullard, E. C. Reversals of the Earth's Magnetic Field. Phil., Trans. Roy. Soc. London, pp. 481-524, 1968.

Cannon, W. F. & Gair, E. "A Revision of Stratigraphic Nomenclature for Middle Precambrian Rocks in Northern Michigan." Geological Society of America Bulletin, vol. 81, pp. 2843-2846, 1970.

Carmichael, R. S. "Geophysical Prospecting Field Manual." Department of Geology, Michigan State University, pp. 4-8b, 1974.

Charles, E. J. "Magnetization of Keweenawan Rocks near Culuth, Minnesota." Geophysics, vol. XXX, no. 5, pp. 858-874, 1965.

David, P. Sur la stabilité de la direction d'aimantation dans quelques roches volcaniques. C. R. Acad. Sci., Paris, 1904.

Department of the Interior, U.S.G.S. Prepared in cooperation with the Michigan Department of Natural Resources, Geological Survey Division. "Aeromagnetic Map of the Menominee-Northland Area, Dickinson, Marquette, and Menominee Counties, Michigan, and Marinette County, Wisconsin." Geophysical Investigations, Map GP-711, published by the U.S.G.S., 1970.

Dobrin, M. B. Introduction to Geophysical Prospecting. 2nd ed. New York: McGraw-Hill Book Co., 1960.

Frederik, B. P. "Remanent Magnetism and the Anomaly at Cottoner Mountain, Madison County, Missouri." Geophysics, vol. 33, no. 4, pp. 613-620, 1968.

Garland, G. D. "Combined Analysis of Gravity and Magnetic Anomalies." Geophysics, vol. 16, pp. 51-62, 1951.

Girdler, R. W. & Peter, G. "An Example of the Importance of Natural Remanent Magnetization in the Interpretation of Magnetic Anomalies." Geophysical Prospecting, vol. VIII, pp. 474-483, 1960.

Green, R. "Remanent Magnetization and the Interpretation of Magnetic Anomalies." Geophysical Prospecting, vol. 8, pp. 98-110, 1960.

Hammer, S. "Approximate Gravity Calculations." Geophysics, vol. 39, pp. 205-222, 1974.

Heiland, C. A. Geophysical Exploration. New York: Prentice Hall, Hener Publishing Co., 1968.

Hinze, W. J. "Geophysical Studies of Basement Geology of Southern Peninsula of Michigan." Am. Assoc. Pet. Geol. Bull., vol. 59, no. 9, pp. 1562-1584, 1975.

Jakosky, J. J. Exploration Geophysics. Trija Publishing Co., pp. 160-165, 1961.

John, S. K. & Cannon, F. "Geological Interpretation of Gravity Profiles in the Western Marquette District, Northern Michigan." Geological Society of America Bulletin, vol. 85, pp. 213-218, 1974.

Larson, E. E. & Strangway, D. W. "Magnetic Polarity and Igneous Petrology." Nature, pp. 756-7, 1966.

Leith, C. K. & Allen, R. C. "Discussion of Correlation of the Huronian Group of Michigan and the Lake Superior." Journal of Geology, vol. 23, pp. 716, 1915.

McElhinny, M. W. Paleomagnetism and Plate Tectonics. Cambridge University Press, 1973.

Meshref, W. M. & Hinze, W. J. "Geologic Interpretation of Aeromagnetic Data in Western Upper Peninsula of Michigan." Michigan Geological Survey, Report of Investigation, 12, 1970.

Nagata, T. Rock Magnetism. Tokyo: Maruzen Co., Ltd., 1961.

Nettleton, L. L. Geophysical Prospecting for Oil. New York: McGraw-Hill Co., 1940.

Nettleton, L. L. "Gravity and Magnetics Calculation." Geophysics, vol. 7, pp. 293-310, 1942.

Nettleton, L. L. Society of Exploration Geophysicists, Elementary Gravity and Magnetics for Geologists and Scismologists, Monograph Series No. 1, Tulsa, Oklahoma, 1971.

Parasnis, D. S. Mining Geophysics. Elsevier Scientific Publishing Co., 1975.

Parasnis, D. S. Principles of Applied Geophysics. London: Chapman and Hall, Ltd., 1972.

Peters, L. J. "The Direct Approach to Magnetic Interpretation and Its Practical Applications." Geophysics, vol. 14, pp. 290-320, 1949.

Russell, I. C. "The Surface Geology of Portions of Menominee, Dickinson, and Iron Counties." Geological Survey, Michigan, Annual Report, pp. 7-82, 1906.

Scheidegger, A. E. Foundations of Geophysics. Elsevier Scientific Publishing Co., New York, 1976.

Shurbet, D. H. et al. "Remanent Magnetization from Comparison of Gravity and Magnetic Anomalies." Geophysics, vol. 41, no. 1, pp. 56-60, 1976.

Singh, C. L. & Ram, A. "A Study of the Vertical Magnetic Anomaly Caused by Magnetite Deposits in Sua Area of Palamau District Bihar (India)." Pure and Applied Geophysics, vol. 85, pp. 283-289, 1971.

Smellie, D. W. "Elementary Approximations in Aeromagnetic Interpretation." Geophysics, vol. 21, pp. 1021-1040, 1956.

Strangway, D. W. History of the Earth's Magnetic Field, Earth and Planetary Science Series. New York: McGraw-Hill Co., 1970.

Vacquier, V. et al. "Interpretation of Aeromagnetic Maps. Memoir, 47 of The Geological Society of America, pp. 6-7, 1951.

Vanlier, K. E. "Ground-Water in Menominee County." Michigan Geological Survey Section, Department of Conservation, 1963.

Verma, R. K. et al. "Results of Vertical Magnetometer Surveys over Raniganj Coalfield, India." Geophysics Research Bulletin, vol. 11, no. 3, pp. 167-168, 1973.

Watkings, N. D. & Haggerty, S. E. "Oxidation and Magnetic Polarity in Single Icelandic Lavas and Dykes." Geophysics. J. Roy. Astron. Soc., 15, pp. 305-15, 1968.

William, B. W. "Textural Variation within a Quartz Diorite Pluton (Twelve-foot Falls Pluton), Northeastern Wisconsin." Geological Society of America Bulletin, vol. 74, pp. 243-250, 1963.